

## Translocation of the nonlabeled antimicrobial peptide PGLa across lipid bilayers and its entry into vesicle lumens without pore formation

メタデータ	言語: eng 出版者: 公開日: 2023-02-21 キーワード (Ja): キーワード (En): 作成者: Ali, Md.Hazrat, Shuma, Madhabi Lata, Dohra, Hideo, Yamazaki, Masahito メールアドレス: 所属:
URL	<a href="http://hdl.handle.net/10297/00029374">http://hdl.handle.net/10297/00029374</a>

# **Translocation of the Nonlabeled Antimicrobial Peptide PGLa across Lipid Bilayers and its Entry into Vesicle Lumens without Pore Formation**

Md. Hazrat Ali,<sup>a</sup> Madhabi Lata Shuma,<sup>a,§</sup> Hideo Dohra,<sup>b,c</sup>

and Masahito Yamazaki<sup>a, c, d, e, \*</sup>

<sup>a</sup> *Integrated Bioscience Section, Graduate School of Science and Technology, Shizuoka University, Shizuoka 422-8529, Japan,* <sup>b</sup> *Instrumental Research Support Office, Research Institute of Green Science and Technology,* <sup>c</sup> *Department of Science, Graduate School of Integrated Science and Technology, Shizuoka University, Shizuoka 422-8529, Japan,* <sup>d</sup> *Nanomaterials Research Division, Research Institute of Electronics, Shizuoka University, Shizuoka 422-8529, Japan,* <sup>e</sup> *Department of Physics, Faculty of Science, Shizuoka University, Shizuoka 422-8529, Japan*

<sup>§</sup>Present address: Department of Pharmacy, Stamford University Bangladesh, Ramna, Dhaka-1217,

Bangladesh

**\*Correspondence should be addressed to:**

Dr. Masahito Yamazaki

Nanomaterials Research Division, Research Institute of Electronics

Shizuoka University

836 Oya, Suruga-ku, Shizuoka 422-8529, Japan

Tel/Fax: 81-54-238-4741

E-mail: [yamazaki.masahito@shizuoka.ac.jp](mailto:yamazaki.masahito@shizuoka.ac.jp)

## ABSTRACT

Fluorescent-probe-labeled peptides are used to study the interactions of peptides with cells and lipid vesicles but labeling peptides with fluorescent probes can significantly change these interactions. We recently developed a new method to detect the entry of nonlabeled peptides into the lumen of single giant unilamellar vesicles (GUVs). Here we applied this method to examine the interaction of the antimicrobial peptide PGLa with single GUVs to elucidate whether PGLa can enter the GUV lumen without pore formation. First, we examined the interaction of nonlabeled PGLa with single GUVs comprising dioleoylphosphatidylglycerol (DOPG) and dioleoylphosphatidylcholine (DOPC) (4/6) whose lumens contain the fluorescent probe AF647 and DOPG/DOPC (8/2)-large unilamellar vesicles encapsulating a high concentration of calcein. After a large lag period from starting the interaction with PGLa, the fluorescence intensity of the GUV lumen due to calcein ( $I_{\text{calcein}}$ ) increased gradually without leakage of AF647, indicating that PGLa enters the GUV lumen without pore formation in the GUV membrane. The fraction of entry of PGLa increased with increasing PGLa concentration. Simultaneous measurement of the fractional area change of the GUV membrane ( $\delta$ ) and PGLa-induced increase in  $I_{\text{calcein}}$  showed that the entry of PGLa occurs only during the second increase in  $\delta$ , indicating that PGLa enters the lumen during its translocation from the outer leaflet to the inner leaflet. The fraction of entry of PGLa without pore formation increased with increasing membrane tension. Based on these results, we discuss the elementary processes and the mechanism of the entry of PGLa into the GUV lumen.

**Key words;** antimicrobial peptides, PGLa, translocation, entry, pore formation, giant unilamellar vesicle

## 1. Introduction

Antimicrobial peptides (AMPs) are gene-encoded and synthesized in the ribosomes of almost all multicellular organisms to provide a first line of defense against bacteria and fungi.<sup>1-5</sup> Most AMPs are highly positively charged short peptides<sup>1-6</sup> and are generally divided into two categories: type A and type B. Type A AMPs damage the plasma membrane of bacterial cells through pore formation, inducing rapid leakage of the internal cell contents<sup>7,8</sup> and include LL-37, magainin 2, and lactoferricin B (LfcinB). Type B AMPs enter the cytosol of bacterial cells without damaging the plasma membrane (i.e., without significant leakage) and bind to the DNA or proteins in the cytoplasm. Buforin II and a short fragment of LfcinB, LfcinB (4-9), belong to the type B category.<sup>9,10</sup>

PGLa is an AMP produced by the African clawed frog *Xenopus laevis*.<sup>11,12</sup> PGLa is a 21 amino acid residue peptide with the sequence GMASKAGAIAGKIAKVALKAL-NH<sub>2</sub>. Positively charged PGLa can bind to negatively charged lipid bilayers due to electrostatic attraction.<sup>13,14</sup> Studies using circular dichroism spectroscopy indicate that PGLa has a random coil structure in aqueous solution but it forms an  $\alpha$ -helix after binding to lipid membranes.<sup>13,15</sup> The structure and orientation of PGLa in lipid bilayers have been extensively investigated using NMR.<sup>16-19</sup> PGLa forms an  $\alpha$ -helix at the membrane interface, and at low peptide concentrations, the tilt angle of the  $\alpha$ -helix (defined by the angle of the membrane normal and the  $\alpha$ -helix axis) is 98° (i.e., almost parallel with the membrane surface) (S-state). However, at higher concentrations the  $\alpha$ -helix is inserted obliquely into the membrane hydrophobic core, with a tilt angle of 126° (T-state). Studies using suspensions of large unilamellar vesicles (LUVs) indicate that PGLa induces leakage of water-soluble fluorescent dyes from the LUVs.<sup>20-23</sup> Moreover, a study using the single giant unilamellar vesicle (GUV) method indicates that PGLa forms pores in lipid bilayers, resulting in the leakage of entrapped fluorescent probes.<sup>24</sup> These results suggest that PGLa may belong to the type A category.

The location of PGLa during PGLa-induced pore formation has been investigated by studying the interaction of a mixture of PGLa and a very low concentration of the fluorescent probe carboxyfluorescein (CF)-labeled PGLa (CF-PGLa) with single GUVs.<sup>24</sup> The fractional area change  $\delta$  of the GUV membrane was found to increase with time in two steps: an increase in  $\delta$  to a steady value,  $\delta_1$ , which remains constant for an extended

period, and then another increase to a second steady value,  $\delta_2$ , without pore formation in the GUV membrane. Concomitantly, the fluorescence intensity (FI) of the GUV rim (i.e., rim intensity),  $I_{\text{rim}}$ , due to CF-PGLa also increases with time in a two-step manner, and the time courses of the increase in  $I_{\text{rim}}$  and  $\delta$  are almost the same. During the increase from  $\delta_1$  to  $\delta_2$ , the FI of the GUV lumen due to CF-PGLa increases, indicating that CF-PGLa enters the lumen without pore formation. A very low concentration of CF-PGLa (0.15  $\mu\text{M}$ ) was used in these experiments to monitor the location of CF-PGLa, and thus the change in  $\delta$  is determined by PGLa and the change in  $I_{\text{rim}}$  is determined by CF-PGLa. Two interpretations of these results (or scenarios of the behavior of PGLa) have been proposed.<sup>24</sup> In interpretation A, a structural change in PGLa from structure A (the S-state) to structure B (the T-state) induces the two-step increase in  $\delta$ , and during this structural change only CF-PGLa translocates from the outer leaflet to the inner leaflet due to a large structural fluctuation of the lipid bilayer. Subsequently, CF-PGLa enters the GUV lumen and PGLa locates only in the outer leaflet before pore formation. In this interpretation, the behavior of CF-PGLa in the lipid bilayer and the interaction of CF-PGLa with the lipid bilayer are considered to be different from that of nonlabeled PGLa due to labeling by the fluorescent probe.<sup>24</sup> In interpretation B, the translocation of PGLa from the outer leaflet to the inner leaflet induces the two-step increase in  $\delta$ , and during this translocation a low concentration of CF-PGLa also translocates in the same manner as PGLa. Labeling peptides with fluorescent probes generally affects the interaction of the peptides such as cell-penetrating peptides (CPPs) with plasma membranes and lipid bilayers, the entry of the peptides into the cytosol, and the location of the peptides in the cytoplasm.<sup>25,26</sup> Thus, it is highly possible that the labeling of PGLa with a fluorescent probe may change the interaction of PGLa with lipid bilayers and its behavior in lipid vesicles. If this is the case, then interpretation A is more satisfactory. Generally, CPPs have an activity to enter the cytosol, but they are used with the labeling of fluorescent probes and biological cargo.<sup>27-31</sup> In contrast, AMPs such as PGLa exhibit activity in bacterial cells even when not labeled with fluorescent probes. It is therefore important to examine the interaction of nonlabeled AMPs with lipid bilayers. Several recent reports describe molecular dynamics (MD) simulations at the all-atom level of the translocation of non-fluorescently labeled peptides across lipid bilayers,<sup>32-34</sup> whereas most experiments on the translocation of peptides have used fluorescent probe-labeled peptides. Therefore, comparison of experimental with MD simulation results requires

experimental data on the translocation of nonlabeled peptides because fluorescent probes are not attached to peptides in MD simulations.

We recently developed a new method for detecting the entry of nonlabeled peptides into the GUV lumen to study the interaction of CPPs with GUVs.<sup>35</sup> In this method, confocal laser scanning microscopy (CLSM) is used to observe the interaction of CPPs with single GUVs containing LUVs 100 nm in diameter which encapsulate a high concentration of the water-soluble fluorescent dye calcein. If peptides enter the GUV lumen and induce calcein leakage from the LUVs, the FI of the GUV lumen due to calcein ( $I_{\text{calcein}}$ ) increases due to fluorescence dequenching and thus an increase in  $I_{\text{calcein}}$  indicates the entry of peptides into the GUV lumen. In this study, to elucidate the translocation of nonlabeled PGLa across a lipid bilayer and its entry into a lipid vesicle lumen, we examined the interaction of nonlabeled PGLa with single GUVs comprising dioleoylphosphatidylcholine (DOPC) and dioleoylphosphatidylglycerol (DOPG). First, we examined the interaction of PGLa with LUVs composed of DOPG and DOPC and containing a high concentration of calcein in their lumen using the LUV suspension method to determine the optimum conditions of LUVs in a GUV lumen. Second, we used CLSM to investigate the interaction of PGLa with single DOPG/DOPC (4/6, molar ratio)-GUVs containing DOPG/DOPC (8/2)-LUVs and another water-soluble fluorescent probe, Alexa Fluor 647 hydrazide (AF647). We found that  $I_{\text{calcein}}$  increased gradually after an initial lag following the starting of the interaction of PGLa with single GUVs without leakage of AF647. This result indicates that PGLa enters the GUV lumen without pore formation in the GUV membranes. Third, to examine the relation between the entry of PGLa into single GUV lumens and the location of PGLa in the GUV membrane, we simultaneously measured the PGLa-induced increase in  $I_{\text{calcein}}$  and the PGLa-induced fractional area change of the GUV membrane ( $\delta$ ), as well as the lumen intensity due to AF647. Finally, we examined the effect of membrane tension on the rate of entry of PGLa into single GUV lumens. Based on the obtained results, we discuss the elementary processes and mechanism of the translocation of nonlabeled PGLa across the GUV membrane and its entry into the GUV lumen.

## **2. Materials and Methods**

### **2.1 Chemicals**

1,2-Dioleoyl-*sn*-glycero-3-phosphocholine (DOPC or 18:1 ( $\Delta^9$ -cis) PC) and 1,2-dioleoyl-*sn*-glycero-3-phospho-(1'-*rac*-glycerol) (DOPG or 18:1 ( $\Delta^9$ -cis) PG) were purchased from Avanti Polar Lipids (Alabaster, AL, USA). Bovine serum albumin (BSA) was purchased from FUJIFILM Wako Pure Chemical Co. (Osaka, Japan). AF647 was purchased from Invitrogen (Carlsbad, CA, USA). PGLa was synthesized using an Initiator+ Alstra (Biotage, Uppsala, Sweden) and a 433A peptide synthesizer (PE Applied Biosystems, Foster City, CA, USA) by the FastMoc method. The cleavage, purification using reverse-phase HPLC, and characterization of the peptides using mass spectroscopy were described previously.<sup>24</sup>

## **2.2. Fluorescence spectroscopic measurement of the interaction of PGLa with DOPG/DOPC-LUVs encapsulating calcein**

We investigated the interaction of PGLa with DOPG/DOPC-LUVs encapsulating calcein using the same method as reported previously.<sup>35</sup> DOPG/DOPC-LUVs containing a high concentration of calcein were prepared by the standard extrusion method. First, multilamellar vesicles (MLVs) of DOPG/DOPC were prepared by mixing 70 mM calcein in Milli-Q water (pH 7.0; adjusted with NaOH) containing 0.10 M sucrose with a dry DOPG/DOPC lipid film using a vortex mixer at room temperature. After subjecting the MLV suspension to three freeze-thaw cycles, the suspension was extruded by passing through a 100 nm pore polycarbonate membrane using a standard procedure. The LUVs were purified by removing free calcein outside the LUVs using gel chromatography with a Sephadex G-75 column and eluting with buffer A (10 mM PIPES, pH 7.0, 150 mM NaCl, and 1 mM EGTA) containing 0.10 M sucrose. Lipid concentrations in the LUV suspensions were determined using the Bartlett method.<sup>36</sup>

Fluorescence measurements of the interaction of PGLa with DOPG/DOPC-LUVs were performed using a fluorescence spectrophotometer (F-7000, Hitachi, Tokyo, Japan). The temperature of the samples was controlled at 25 °C by a water bath circulator.<sup>35</sup> The excitation and emission wavelengths were 490 nm and 520 nm, respectively, and the excitation and emission slits were both 2.5 nm. The time course of the fluorescence intensity (FI) change of a DOPG/DOPC-LUV suspension after starting the interaction with various concentrations of PGLa in buffer A containing 0.1 M sucrose was monitored for a specific time (i.e., 6 min). The percent leakage of calcein from LUVs induced by the interaction with PGLa was calculated by setting the

FI of the LUV suspension after interaction with 0  $\mu\text{M}$  PGLa to 0%, and that after interaction with Triton X-100 (final concentration of 0.9% (v/v)) to 100%. The FI of the LUV suspensions after interaction with PGLa for 6 min was determined by subtracting the FI of the LUV suspension without interaction with PGLa (i.e., the FI increase or the increment of FI).

### 2.3. GUV preparation

We prepared DOPG/DOPC (4/6, molar ratio)-GUVs (hereafter DOPG/DOPC (4/6)-GUVs) containing DOPG/DOPC (8/2)-LUVs (encapsulating a high concentration of calcein) inside the GUV lumen in buffer A containing 0.10 M sucrose and 6  $\mu\text{M}$  AF647 using the natural swelling method.<sup>35,37,38</sup> First, a pre-hydrated DOPG/DOPC film was incubated in buffer A containing 0.10 M sucrose, a suspension of purified DOPG/DOPC (8/2)-LUV (encapsulating calcein), and AF647 (final concentration of lipids and AF647 were 12.5  $\mu\text{M}$  and 6.0  $\mu\text{M}$ , respectively) at 37 °C for 2 h. These GUVs were purified by removing unencapsulated LUVs and AF647 by filtering through a 10  $\mu\text{m}$  pore-size nucleopore membrane in buffer A containing 0.1 M glucose.<sup>39</sup> After purification, the buffer outside the GUVs was 0.10 M glucose in buffer A and that inside the GUVs was 0.10 M sucrose in buffer A. Since the efficiency of LUV entrapment in a GUV lumen is 81%,<sup>35</sup> the lipid concentration due to the LUVs in the lumen of the GUVs prepared above is estimated to 10  $\mu\text{M}$ .

### 2.4. Single GUV method to monitor interaction of PGLa with DOPG/DOPC-GUVs containing LUVs

A GUV suspension purified using the procedure described in section 2.3 was transferred into a hand-made microchamber.<sup>35</sup> Then a confocal laser scanning microscope (FV-1000, Olympus, Tokyo, Japan) equipped with a 60 $\times$  objective (UPLSAPO060X0, Olympus) was used to observe the interaction of PGLa with single DOPG/DOPC (4/6)-GUVs 20–40  $\mu\text{m}$  in diameter containing AF647 and LUVs (encapsulating calcein). A 633 nm laser was used to excite AF647 and a 488 nm laser was used to excite calcein to obtain CLSM images of the GUVs<sup>35</sup> at  $25 \pm 1$  °C (controlled by a ThermoPlate, Tokai Hit, Shizuoka, Japan). The inner glass surfaces of the microchamber were coated with BSA to eliminate strong interactions between the GUVs and the glass surfaces.

The interaction of PGLa with a target GUV was started by introducing a PGLa solution (in buffer A containing 0.10 M glucose) to the vicinity of the GUV using a 20  $\mu\text{m}$  in diameter micropipette and positive pressure (30 Pa). The distance between the micropipette tip and the target GUV was  $\sim 50 \mu\text{m}$ .<sup>40</sup> The PGLa concentration in the vicinity of the target GUV was 78% of that in the micropipette under the experimental conditions used<sup>40</sup> and this concentration was used to obtain the corrected PGLa concentrations near the GUV, as described below.

The FI due to AF647 and that due to calcein in a GUV lumen were obtained by measuring the FI of a circle (with a diameter  $\sim 50\%$  that of the GUV) located at the center of the GUV, and then these FI values were corrected by subtracting the FI outside the GUV prior to interaction with the PGLa solution.

## **2.5. Measurement of PGLa-induced fractional area change of GUV membrane during entry of PGLa into GUV lumen**

We observed the interaction of PGLa with a GUV held by a micropipette (micropipette A, coated with BSA) using a slight suction pressure under the confocal laser scanning microscope.<sup>40</sup> First, DOPG/DOPC (4/6)-GUVs containing LUVs (encapsulating calcein) and AF647 suspension were prepared and purified as described in section 2.3. A single GUV was then transferred to the microchamber and held by micropipette A ( $\sim 10 \mu\text{m}$  in diameter) using suction pressure, inducing a tension in the GUV membrane of 0.50 mN/m for 2 min. The tension on the GUV,  $\sigma$ , was controlled by the suction pressure,  $\Delta P (= P_o - P_i)$ , where  $P_o$  and  $P_i$  are the pressures outside and inside micropipette A, respectively.<sup>41</sup>

$$\sigma = \frac{\Delta P d_p}{4(1 - d_p/D_V)} \quad (1)$$

in which  $d_p$  is the internal diameter of micropipette A and  $D_V$  is the diameter of the spherical part (outside the micropipette) of the GUV held by the micropipette. Next, a PGLa solution was continuously added through a micropipette 20  $\mu\text{m}$  in diameter, micropipette B, to the vicinity of the GUV by applying a positive pressure inside micropipette B ( $P_i - P_o = 30 \text{ Pa}$ ). The separation between the GUV and the tip of micropipette B was  $\sim 40 \mu\text{m}$ . Under this condition, the PGLa concentration in the vicinity of the target GUV was 58% of that in

micropipette B.<sup>40</sup> The corrected PGLa concentrations in the vicinity of the GUV based on this measurement are described below. We measured the fractional area change of the GUV membrane,  $\delta = \Delta A/A_0$ , where  $A_0$  is the initial area of a GUV before starting the interaction with PGLa and  $\Delta A$  is the area change of the GUV membrane during its interaction with PGLa, using the following equation:<sup>41</sup>

$$\delta = \frac{d_p \Delta L (1 - d_p/D_v)}{D_{v0}^2} \quad (2)$$

in which  $\Delta L$  is the projection length change of the GUV inside micropipette A.

The FI values due to AF647 and to calcein in a GUV lumen were obtained as described in section 2.4.

## 2.6. Effect of membrane tension on entry of PGLa into GUV lumen

We used the method described in section 2.5 but applied various membrane tensions (0.50–1.5 mN/m) to the GUV using different suction pressures in micropipette A.

## 2.7. Detection of the minimum PGLa concentration in a GUV lumen

The minimum PGLa concentration in DOPG/DOPC (4/6)-GUV lumens detected by the present method was estimated as follows.<sup>35</sup> First, the interaction of 10  $\mu$ M DOPG/DOPC (8/2)-LUVs with various concentrations of PGLa was monitored for 6 min using the fluorescence spectrophotometer by the method of section 2.2, Then the LUV suspension was transferred to a microchamber and observed at 15  $\mu$ m above the upper surface of the cover slip using CLSM. The FI values of 6 circles 20  $\mu$ m in diameter were measured using the same CLSM conditions for the measurement of the GUVs (section 2.4), and the mean values were obtained.

# 3. Results and Discussion

## 3.1. PGLa-induced calcein leakage from DOPG/DOPC-LUVs

The entry of peptides into a DOPG/DOPC (4/6)-GUV lumen was previously detected using 100 nm in diameter LUVs encapsulating a high concentration of calcein. After interaction with the peptides, the calcein is released from the LUV lumen, resulting in an increase in the FI of the GUV lumen.<sup>35</sup> To increase the efficiency

of detection, we needed to optimize the DOPG concentration in the LUV membranes and the lipid concentration in the GUV lumen by considering that (i) the efficiency of peptide-induced leakage from LUVs is higher than that from GUVs, and (ii) the entry of peptides induces a large increase in the FI of the GUV lumen. We thus selected DOPG/DOPC (8/2)-LUVs because the binding constant of PGLa to DOPG/DOPC-LUVs increases with DOPG concentration due to electrostatic interactions between cationic PGLa and anionic DOPG/DOPC membranes,<sup>13,15</sup> and also because the interaction of the peptide TP10 with DOPG/DOPC-LUVs (specifically, DOPG/DOPC (8/2)) provides the highest rate of leakage.<sup>35</sup> To obtain the optimum lipid concentration, we investigated the interaction of PGLa with DOPG/DOPC (8/2)-LUVs encapsulating a high concentration of calcein using the LUV suspension method as follows.

The FI of a suspension of 10  $\mu\text{M}$  DOPG/DOPC (8/2)-LUVs was initially very low due to fluorescence quenching, then increased gradually with time after starting the interaction of PGLa with the LUVs. We converted the FI to the fraction of calcein leakage compared to total leakage (%) to obtain the efficiency of leakage. The fraction of PGLa-induced calcein leakage increased with time for the 6-min measurement period using 0.60 to 2.0  $\mu\text{M}$  PGLa, and the fraction of leakage increased as the PGLa concentration increased (Fig. 1A). There was no significant calcein leakage at and below 0.40  $\mu\text{M}$  PGLa. We obtained similar results in two independent experiments ( $N = 2$ ), indicating that the results are reproducible. The PGLa-induced leakage (%) and the FI of the suspension at 6 min increased with an increase in PGLa concentration from 0.60 to 2.0  $\mu\text{M}$  (Fig. 1B).

The fraction of AMP-induced leakage from LUVs in suspension reportedly depends greatly on the lipid concentration in the LUV suspension<sup>35</sup> and thus we investigated the effect of lipid concentration (or LUV concentration) on PGLa-induced calcein leakage. The fraction of calcein leakage (%) from the LUVs after 6 min of interaction with 1.0  $\mu\text{M}$  PGLa increased as the lipid concentration decreased, and the FI increase of the suspension under the same conditions was maximum at 10  $\mu\text{M}$  lipid (Fig. 1C). These results are consistent with those reported previously.<sup>35</sup> The dependence of the FI increase on lipid concentration can be explained by the total amount of calcein in the LUV suspension and the fraction of leakage.<sup>35</sup>

We conducted experiments to determine the dependence of the FI of a LUV suspension on lipid concentration using different PGLa concentrations. At all examined concentrations, we observed a maximum

Figure 1

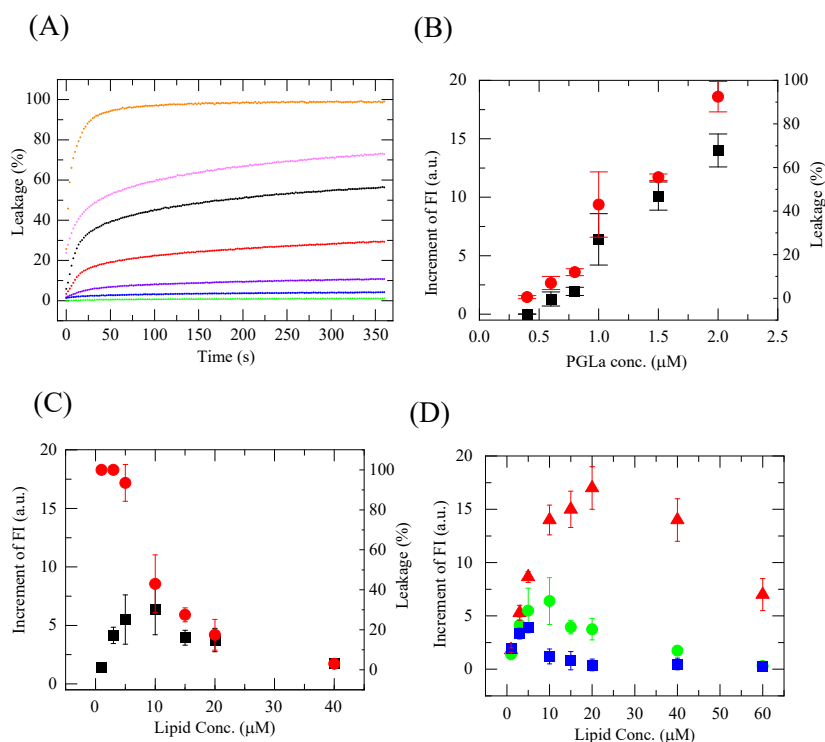


Figure 1: PGLa-induced calcein leakage from DOPG/DOPC (8/2)-LUVs in their suspension. (A) Time course of change in calcein leakage (%) from the LUVs during the interaction of various concentrations of PGLa at 25 °C. PGLa solutions were mixed with the LUV suspension at time,  $t = 0$ . Final PGLa concentrations in the samples are 2.0  $\mu\text{M}$  (orange line), 1.8  $\mu\text{M}$  (pink), 1.5  $\mu\text{M}$  (black), 1.0  $\mu\text{M}$  (red), 0.8  $\mu\text{M}$  (violet), 0.6  $\mu\text{M}$  (blue), and 0.4  $\mu\text{M}$  (green) PGLa from the top. Lipid concentration of the LUV suspensions was 10  $\mu\text{M}$ . (B) PGLa concentration dependence of the fraction of calcein leakage (%) at 6 min interaction and the FI increase of the LUV suspension under the same condition. These data were obtained by the analysis of the experiments shown in panel A. Mean values and SDs ( $N = 2-4$ ) of leakage (%) (red ●) and FI increase (■) are shown. (C) Lipid concentration dependence of fraction of 1.0  $\mu\text{M}$  PGLa-induced calcein leakage (%) from the LUVs at 6 min interaction, and of the FI increase of their suspension. Mean values and SDs ( $N = 2-4$ ) of leakage (%) (red ●) and FI increase (■) are shown. (D) Lipid concentration dependence of FI increase of a suspension of the LUVs after interaction with various concentrations of PGLa for 6 min. Mean values and SDs ( $N = 2-4$ ) of FI increase are shown; 2.0  $\mu\text{M}$  (red ▲), 1.0  $\mu\text{M}$  (green ●), and 0.5  $\mu\text{M}$  (blue ■) PGLa.

in FI increase, which became higher with increasing PGLa concentration (Fig. 1D). The FI increase at 10  $\mu\text{M}$  lipid ranged from 0 to 14 for concentrations of PGLa  $\leq 2.0$   $\mu\text{M}$ , and the FI increase had a large dynamic range (i.e., the ratio of the maximum to the minimum) of 5.3 from 0.5 to 1.0  $\mu\text{M}$  PGLa and of 2.2 from 1.0 to 2.0  $\mu\text{M}$  PGLa (thus, a dynamic range of 12 from 0.5 to 2.0  $\mu\text{M}$  PGLa). Therefore, a lipid concentration of 10  $\mu\text{M}$  was selected to detect the entry of PGLa into a GUV lumen.

### 3.2. Entry of nonlabeled PGLa into single DOPG/DOPC-GUV lumen

To examine the entry of PGLa into a GUV lumen, we prepared DOPG/DOPC (4/6)-GUVs containing AF647 and 10  $\mu\text{M}$  DOPG/DOPC (8/2)-LUVs in the GUV lumen, where the LUVs contained a high concentration of calcein. We then investigated the interaction of nonlabeled PGLa with single DOPG/DOPC (4/6)-GUVs using the single GUV method. A target GUV was selected under a confocal laser scanning microscope, and then a solution of PGLa was added to the vicinity of the GUV through a micropipette. The PGLa concentration near the GUV immediately reached a steady value, similar to the concentration in the micropipette, and remained constant during the interaction because of continuous addition of PGLa from the micropipette.<sup>40</sup> First we examined the interaction of single GUVs with 2.9  $\mu\text{M}$  PGLa. The FI of the GUV lumen due to AF647 (i.e.,  $I_{\text{AF647}}$ ) remained constant during the 6 min of interaction (Fig. 2A (2) and Fig. 2B, red curve). This result shows that AF647 does not leak through the GUV membrane, indicating that no pore formation occurs in the GUV membrane under this condition. In contrast, initially the FI of the GUV lumen due to calcein ( $I_{\text{calcein}}$ ) was very low, indicating no leakage from the LUVs.  $I_{\text{calcein}}$  started to increase at 134 s, increased gradually with time for 90 s, and reached a steady, maximum, value (Fig. 2A (1) and Fig. 2B, green curve). We can explain these observations as follows.<sup>35</sup> The interaction of PGLa with a single GUV induces the translocation of PGLa across the GUV membrane from the outer leaflet to the inner leaflet, then PGLa enters the GUV lumen without pore formation in the GUV membrane. Subsequently, PGLa in the GUV lumen induces calcein leakage from the LUVs after the PGLa concentration in the GUV lumen reaches a threshold concentration (0.6  $\mu\text{M}$ ). The leaked calcein molecules in the GUV lumen elevate  $I_{\text{calcein}}$  due to the dequenching of calcein fluorescence. The experiment was repeated using 12 single GUVs. Similar results (i.e.,  $I_{\text{calcein}}$  increases without membrane permeabilization of AF647) were obtained with 8 GUVs, but with 4 GUVs  $I_{\text{calcein}}$  did not increase significantly. As shown in Fig. 2C, the onset time to start an increase in  $I_{\text{calcein}}$  differed, but in most GUVs  $I_{\text{calcein}}$  reached a steady, maximum value at 80–100 s after the start of increase whereas in some GUVs  $I_{\text{calcein}}$  did not reach a steady, maximum by 6 min, and in the other GUVs no increase in  $I_{\text{calcein}}$  occurred.

If the PGLa-induced increase in  $I_{\text{calcein}}$  is large, it is easy to conclude that PGLa enters the GUV lumen, but if the increase is small, we need a threshold intensity of  $I_{\text{calcein}}$  to judge the entry of PGLa. Under the CLSM conditions used in the PGLa experiments, the threshold intensity was set at 480 because  $I_{\text{calcein}}$  of GUVs

Figure 2

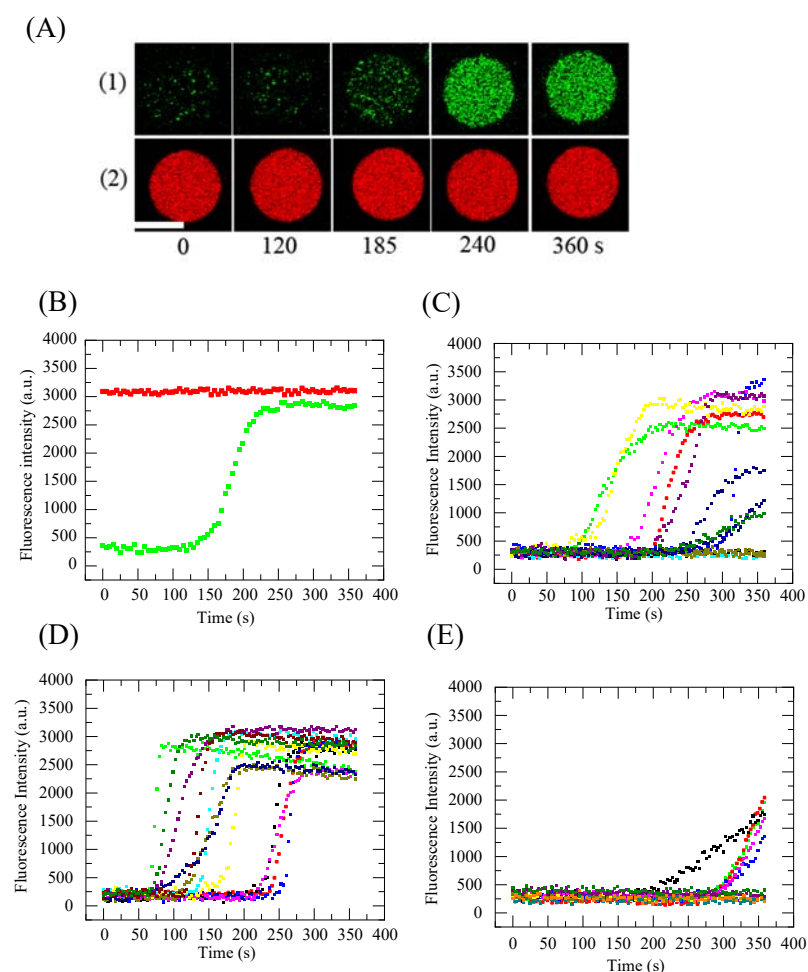


Figure 2. Interaction of  $2.9 \mu\text{M}$  PGLa with a single DOPG/DOPC (4/6)-GUV containing AF647 and  $10 \mu\text{M}$  DOPG/DOPC (8/2)-LUVs in the GUV lumen. These LUVs contained a high concentration of calcein in the LUV lumen, which was sufficiently quenched. (A) CLSM images of the GUV due to (1) calcein and (2) AF 647. The number below each image shows the reaction time between PGLa and the single GUV. Bar,  $30 \mu\text{m}$ . (B) Time course of the change in FI of the GUV shown in panel A. Red curve and green curve correspond to the FI of the GUV lumen due to AF647 ( $I_{\text{AF647}}$ ) and that due to calcein ( $I_{\text{calcein}}$ ), respectively. (C) Other examples of time course of the change in  $I_{\text{calcein}}$  of several GUVs under the same conditions of panel A (interaction with  $2.9 \mu\text{M}$  PGLa). (D) Time course of the change in  $I_{\text{calcein}}$  of several GUVs interacting with  $3.8 \mu\text{M}$  PGLa. (E) Time course of the change in  $I_{\text{calcein}}$  of several GUVs interacting with  $2.3 \mu\text{M}$  PGLa.

containing LUVs (encapsulating calcein) observed at 6 min in the absence of peptides under the same CLSM conditions was  $270 \pm 70$  (the number of examined GUVs,  $n$ , was 9) and thus the mean value of  $I_{\text{calcein}}$  plus 3 times its standard deviation (SD) value is 480. We therefore judged that PGLa entered the GUVs if  $I_{\text{calcein}}$  was higher than 480. One measure of the rate of entry of PGLa into the GUV lumens is the fraction of GUVs into which PGLa enters before 6 min prior to or without pore formation in the GUV membrane (hereafter abbreviated

as the fraction of entry),  $P_{\text{entry}}(6 \text{ min})$ .<sup>37,38,43</sup> The entry of peptides into a single GUV lumen is composed of several elementary processes and some processes occur stochastically, and thus, the entry of peptides into each GUV lumen starts at different time. Therefore, it is difficult to estimate the rate constant of entry of peptides into single GUV lumens at present. The fraction of entry at a specific time,  $P_{\text{entry}}(6 \text{ min})$ , directly represents the rate of increase in the number of GUVs which the peptides enter among the population of the examined GUVs, which increases with an increase in the rate of entry of the peptides into single GUV lumens. Thus, one can regard the fraction of entry as one of the measures of the rate of entry of the peptides. The interaction of 2.9  $\mu\text{M}$  PGLa with single GUVs provided  $I_{\text{calcein}}$  values at 6 min ( $I_{\text{calcein}}(6 \text{ min})$ ) for 8 of the 12 GUVs tested that were higher than the threshold intensity, indicating that in these 8 GUVs PGLa enters their GUV lumen. Thus,  $P_{\text{entry}}(6 \text{ min}) = 0.67$ . Based on the results of two independent experiments ( $N = 2$ ), we obtained a mean value  $\pm$  SD of  $P_{\text{entry}}(6 \text{ min})$  of  $0.68 \pm 0.01$ .

The time required for  $I_{\text{calcein}}$  to begin increasing was different for each GUV, but the time interval required to reach a steady, maximum, value of  $I_{\text{calcein}}$  after the start of increase,  $T_{\text{increase}}$ , was similar ( $90 \pm 30 \text{ s}$ ,  $n = 10$  for  $N = 2$ ). There are two interpretations of the physical meaning of  $T_{\text{increase}}$ . In interpretation A,  $T_{\text{increase}}$  is the approximate period of the entry of PGLa into the GUV lumen because termination of the increase in  $I_{\text{calcein}}$  indicates the end of entry of PGLa. In contrast, interpretation B is based on the idea that termination of the increase in  $I_{\text{calcein}}$  is due to 100% leakage of calcein in the GUV lumen (which means that the PGLa concentration in the lumen reaches 2.0  $\mu\text{M}$ , judging from Fig. 1B). When the PGLa concentration in the GUV lumen is lower than 0.60  $\mu\text{M}$ ,  $I_{\text{calcein}}$  does not increase. Hence, in interpretation B,  $T_{\text{increase}}$  means the time required for the increase in PGLa concentration from 0.60 to 2.0  $\mu\text{M}$ . Thus,  $T_{\text{increase}}$  is a measure of the rate of influx of PGLa.

Next, we performed the same experiments using 3.8  $\mu\text{M}$  PGLa and obtained results similar to that for 2.9  $\mu\text{M}$  PGLa in most GUVs. After a period following the onset of the interaction,  $I_{\text{calcein}}$  started to increase, continued to increase gradually with time, and reached a steady value without leakage of AF647 (Fig. S1 (A) (C) in Supporting Information). This result indicates that PGLa enters the GUV lumen without pore formation in the GUV membrane. However, in some GUVs, after  $I_{\text{calcein}}$  reached a steady value, AF647 and calcein started to leak (Fig. S1 (B) (D) in Supporting Information), indicating that first PGLa enters the GUV lumen and after

a lag period from the time when  $I_{\text{calcein}}$  reaches a steady value, pore formation occurs in the GUV membrane. Two independent experiments gave a  $P_{\text{entry}}$  (6 min) of 1.0. As shown in Fig. 2D, the onset time at which  $I_{\text{calcein}}$  increased differed but reached a steady, maximum, value with similar values of  $T_{\text{increase}}$ . The mean value and standard error (SE) of the steady value of  $I_{\text{calcein}}$  for 3.8  $\mu\text{M}$  PGLa was  $2,700 \pm 400$  ( $n = 24$  for  $N = 2$ ), which is the same as that for 2.9  $\mu\text{M}$  ( $2,800 \pm 300$ ;  $n = 10$  for  $N = 2$ ). This result may indicate that the steady values of  $I_{\text{calcein}}$  for 2.9  $\mu\text{M}$  and 3.8  $\mu\text{M}$  PGLa are the saturated value, suggesting that the fraction of calcein leakage in the GUV lumen interacting with 2.9  $\mu\text{M}$  PGLa may be  $\sim 100\%$ . If this inference is true, these results suggest that the PGLa concentration in the GUV lumen interacting with 2.9  $\mu\text{M}$  PGLa is more than 2.0  $\mu\text{M}$ , given that Fig. 1B shows that the fraction of calcein leakage under the same conditions reaches 100% at 2.0  $\mu\text{M}$  PGLa.  $T_{\text{increase}}$  for 3.8  $\mu\text{M}$  PGLa was  $60 \pm 20$  s ( $n = 22$  for  $N = 2$ ), which is slightly smaller than that for 2.9  $\mu\text{M}$ . This result shows that the rate of influx of PGLa in the interaction with 3.8  $\mu\text{M}$  PGLa is higher than that in the interaction with 2.9  $\mu\text{M}$  PGLa, indicating that the rate of translocation of PGLa is higher in the interaction of 3.8  $\mu\text{M}$  PGLa. The fraction of leaked GUV (hereafter the fraction of leakage) at 6 min,  $P_{\text{leak}}$  (6 min), was  $0.19 \pm 0.01$  ( $N = 2$ ).

We obtained the PGLa concentration dependence of the rate of entry of PGLa into single GUV lumens. Figure 3A shows the mean values of  $P_{\text{entry}}$  (6 min) and  $I_{\text{calcein}}$  (6 min) for all examined GUVs in the interaction with various concentrations of PGLa. The mean values of  $I_{\text{calcein}}$  (6 min) are proportional to the amounts of entered PGLa into single GUV lumen by 6 min interaction, which can also be considered as one of the measures of the rate of entry of peptide into a GUV lumen.<sup>35</sup> As we described later, 0.6  $\mu\text{M}$  is the minimum concentration of PGLa in the GUV lumen detectable using this method (i.e., the threshold concentration for the detection). Thus, we cannot judge the entry of a small amount of PGLa so that its concentration in the GUV lumen is low ( $< 0.6$   $\mu\text{M}$ ). Therefore, we can interpret the results of Fig. 3A as follows. At PGLa concentrations  $\leq 1.2$   $\mu\text{M}$ , no significant entry of PGLa occurred, i.e., the amount of PGLa entered the GUV lumen was zero or small and thus its concentration in the GUV lumen is less than the threshold concentration ( $= 0.6$   $\mu\text{M}$ ). At and above 1.7  $\mu\text{M}$  PGLa,  $P_{\text{entry}}$  (6 min) and  $I_{\text{calcein}}$  (6 min) increased as the PGLa concentration increased. A PGLa concentration range from 1.7  $\mu\text{M}$  to 2.9  $\mu\text{M}$  resulted in significant PGLa entering the GUV lumen without pore formation in the membrane of the GUVs. For 3.8  $\mu\text{M}$  PGLa, pore formation was observed in some GUVs after a lag time

following the entry of PGLa into the GUV lumen, but in most GUVs no pore formation occurred. The rate of entry of PGLa into the GUV lumen increased as the peptide concentration increased. Figure 3B shows that the fraction of leakage of AF647 was 0 at and below 2.9  $\mu\text{M}$ , and 0.19 at 3.8  $\mu\text{M}$  PGLa, indicating that no pore formation occurred in all the GUVs interacting less than 2.9  $\mu\text{M}$  PGLa but pore formation occurred in the membrane of 19% GUVs interacting with 3.8  $\mu\text{M}$  PGLa. At 1.7 and 2.3  $\mu\text{M}$  PGLa,  $I_{\text{calcein}}$  did not reach a steady value by 6 min (Fig. 2E) and thus the value of  $T_{\text{increase}}$  could not be determined.

The minimum PGLa concentration in DOPG/DOPC (4/6)-GUV lumens detected by the present method (i.e., threshold concentration for the detection) was estimated using the same method as reported previously.<sup>35</sup> After 6 min of interaction of 10  $\mu\text{M}$  DOPG/DOPC (8/2)-LUVs with PGLa, the LUV suspension was transferred to a

Figure 3

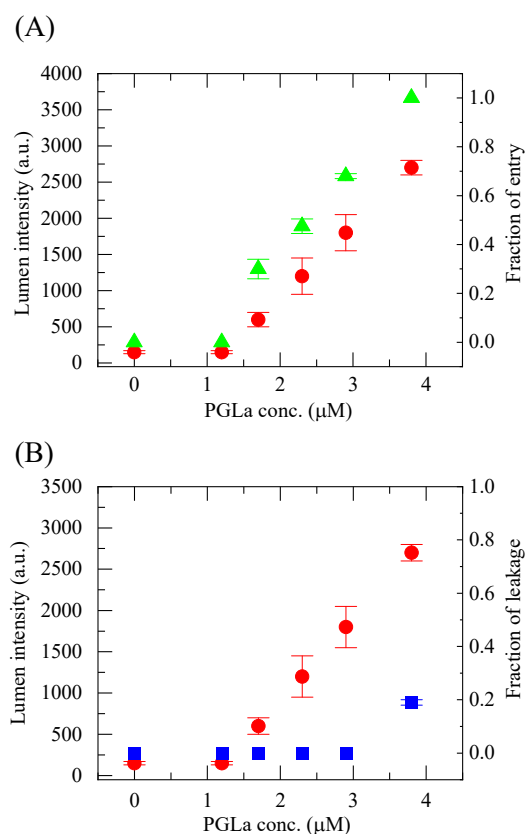


Figure 3. Fraction of entry of nonlabeled PGLa into a GUV lumen. (A) Dependence of  $I_{\text{calcein}}$  (6 min) and the fraction of entry on PGLa concentration. Mean values and SEs ( $N = 2$ ) of  $I_{\text{calcein}}$  (6 min) are shown (red ●). The fraction of entry of PGLa after 6 min interaction,  $P_{\text{entry}}$  (6 min), is also shown (green ▲). (B) Dependence of  $I_{\text{calcein}}$  (6 min) and the fraction of leakage on PGLa concentration. Mean values and SEs ( $N = 2$ ) of  $I_{\text{calcein}}$  (6 min) are shown (red ●). The fraction of leakage of AF647 after 6 min interaction,  $P_{\text{leak}}$  (6 min), is also shown (blue ■).

microchamber and observed at 15  $\mu\text{m}$  above the upper surface of the cover slip using CLSM. Figure S2 shows the dependence of the FI of the LUV suspensions on PGLa concentration. The FI increased with increasing PGLa concentration and saturated at 2.0  $\mu\text{M}$  PGLa. At PGLa concentrations below 0.40  $\mu\text{M}$  the FI values were low, but at 0.60  $\mu\text{M}$  PGLa, the FI (610) value became higher than the threshold intensity (480), indicating that 0.60  $\mu\text{M}$  is the minimum concentration of PGLa in the GUV lumen detectable using this method.

As described in section 3.1, in the method to detect the entry of PGLa into a GUV lumen, to increase the rate of PGLa-induced pore formation in the LUVs than that in the GUVs, we used a higher DOPG mol fraction (or DOPG concentration) in the LUV membrane than that in the GUV membrane because we reasonably expected that the rate of PGLa-induced pore formation in the lipid bilayer increases with an increase in DOPG mol fraction. Therefore, we used the combinations of the DOPG/DOPC (4/6)-GUV containing DOPG/DOPC (8/2)-LUVs. To confirm this concept, we performed the same experiments described in this section using DOPG/DOPC (8/2)-GUV containing DOPG/DOPC (8/2)-LUVs, where the DOPG mol fractions in the GUV membranes and the LUV membranes are the same. Figure S3 shows a typical result of the interaction of 2.9  $\mu\text{M}$  PGLa with a single DOPG/DOPC (8/2)-GUV containing AF647 and 10  $\mu\text{M}$  DOPG/DOPC (8/2)-LUVs in the GUV lumen, where the LUVs contained a high concentration of calcein. After the interaction started, the  $I_{\text{AF647}}$  remained constant by 180 s, then started to decrease (Fig. S3A (2) and Fig. S3B, red curve), indicating that PGLa induced the formation of pores in the GUV membrane and then AF647 leaked out through the pores. In contrast, the  $I_{\text{calcein}}$  started to increase at 160 s, which is 20 s before the onset time of pore formation in the GUV membrane, and increased gradually with time by 240 s, then decreased (Fig. S3A (1) and Fig. S3B, green curve). The value of  $I_{\text{calcein}}$  became a maximum at 60 s later than the onset time of AF647 leakage. These results indicate that first the entry of PGLa into the GUV lumen occurs and then after the PGLa concentration in the GUV lumen increases significantly the formation of pores occurs in the GUV membrane, through which AF647 and calcein leak out. This result provides a similar conclusion obtained using DOPG/DOPC (4/6)-GUV containing DOPG/DOPC (8/2)-LUVs. As reported previously,<sup>24</sup> at the beginning of the PGLa-induced pore formation in the GUVs, the membrane permeability coefficient of calcein is small but it increases with time to a steady, maximum value. Thus, for a short time (60 s) after the pore formation in the GUV membrane, the rate of increase in the calcein concentration in the GUV lumen due to the PGLa-induced release of calcein from the LUVs is

higher than the rate of decrease in calcein concentration due to the membrane permeation of calcein from the GUV lumen to its outside, and thus, the  $I_{\text{calcein}}$  continues to increase. However, after that, the latter rate becomes higher than the former rate and thus the  $I_{\text{calcein}}$  decreases with time. The maximum value of  $I_{\text{calcein}}$  was 1500, which is smaller than the mean, steady value of  $I_{\text{calcein}}$  (2800) observed in the interaction of 2.9  $\mu\text{M}$  PGLa with single DOPG/DOPC (4/6)-GUV containing DOPG/DOPC (8/2)-LUVs. These results indicate that before the  $I_{\text{calcein}}$  reaches a steady value the calcein leakage starts due to the pores in the GUV membrane. Therefore, we cannot obtain the detailed information on the time course of the entry of PGLa. The experiment was repeated using 10 single GUVs. Similar results (i.e., the  $I_{\text{calcein}}$  starts to increase before or at the onset time of the pore formation in the GUV membrane, and reaches a maximum after the pore formation, then decreases) were obtained with 7 GUVs (Figs. S3B and S3C), but with 3 GUVs the  $I_{\text{calcein}}$  did not increase significantly whereas the  $I_{\text{AF647}}$  remained constant (Fig. S3D). The fraction of leakage of AF647 in the interaction of 2.9  $\mu\text{M}$  PGLa with single DOPG/DOPC (8/2)-GUVs was  $0.70 \pm 0.00$  ( $N = 2$  each using 10 GUVs) under this condition, indicating that the rate of PGLa-induced pore formation in the DOPG/DOPC (8/2)-GUVs is much higher than that in the DOPG/DOPC (4/6)-GUVs where the fraction of leakage of AF647 was 0, i.e., no pore formation in all the GUVs (Fig. 3B). This result supports the above concept that the rate of PGLa-induced pore formation in the lipid bilayer increases with an increase in DOPG mol fraction. However, as shown in Fig. 1B, 2.0  $\mu\text{M}$  PGLa can induce 100% leakage from DOPG/DOPC (8/2)-LUVs, and thus, the rate of PGLa-induced pore formation in the DOPG/DOPC (8/2)-LUVs is a little higher than that in the DOPG/DOPC (8/2)-GUVs. This result on the vesicle radius dependence of the rate of peptide-induced pore formation is similar to that of transportan 10 (TP10)-induced pore formation,<sup>35</sup> and the possible causes were discussed previously.<sup>35</sup> Therefore, we conclude that the higher rate of PGLa-induced pore formation in DOPG/DOPC (8/2)-LUVs than that in DOPG/DOPC (4/6)-GUVs can be explained by two factors; one is the higher DOPG mol fraction and the other is the vesicle radius. For the detection method of the entry of peptide into single GUVs, the usage of DOPG/DOPC (4/6)-GUVs containing DOPG/DOPC (8/2)-LUVs is much better than that of GUVs and LUVs with the same mol fraction of DOPG because the rate of PGLa-induced pore formation in DOPG/DOPC (8/2)-LUVs is much higher than that in DOPG/DOPC (4/6)-GUVs, and thus one can observe the detailed time course of entry before pore formation in the GUV membrane.

### 3.3. Relationship between entry of nonlabeled PGLa into GUV lumen and its induced increase in area of GUV membrane

The interaction of PGLa with a single GUV reportedly induces a two-step increase in the area of the GUV membrane without pore formation.<sup>24</sup> We examined the relationship between the entry of nonlabeled PGLa into single GUV lumens and the PGLa-induced incremental increase in the area of the GUV membrane by simultaneously measuring the PGLa-induced increase in the lumen intensity due to calcein ( $I_{\text{calcein}}$ ), the PGLa-induced fractional area change of the GUV membrane ( $\delta$ ), and the lumen intensity due to AF647 ( $I_{\text{AF647}}$ ). We prepared the same GUVs as used in the previous section (i.e., DOPG/DOPC (4/6)-GUVs containing AF647 and 10  $\mu\text{M}$  DOPG/DOPC (8/2)-LUVs encapsulating a high concentration of calcein in the GUV lumen) and examined the interaction of PGLa with a GUV held by a micropipette exerting a membrane tension of 0.5 mN/m.<sup>24,40</sup>

First, we examined the interaction of 2.9  $\mu\text{M}$  PGLa with single DOPG/DOPC (4/6)-GUVs held by a micropipette and obtained two types of the results. Figures 4A and 4B show typical results, here termed pattern A responses.  $I_{\text{AF647}}$  did not change during the interaction (Figs. 4A and 4B, red squares), indicating no pore formation in the GUV membrane. Figure 4B indicates that the  $\delta$  of the GUV rapidly increased to a steady value of  $\delta_1$  at 49 s and remained constant for an extended period (33 s). Then, at 82 s,  $\delta$  started to increase gradually and reached a second steady value of  $\delta_2$  at 175 s, which remained constant up to 6 min. The ratio of  $\delta_2$  to  $\delta_1$  ( $\delta_2/\delta_1$ ) was 2.2. On the other hand,  $I_{\text{calcein}}$  did not increase at the beginning of the interaction but started to increase at 90 s (the onset time in increase in  $I_{\text{calcein}}$ ), which is slightly later than the onset time of the increase in  $\delta$  from the first steady value. Then,  $I_{\text{calcein}}$  reached a steady value at 180 s (the termination time in increase in  $I_{\text{calcein}}$ ), which is similar to the time when  $\delta$  reached the second steady value,  $\delta_2$  (the termination time in increase in  $\delta$ ) (Fig. 4B). These results indicate that PGLa enters the GUV lumen when the GUV membrane area increases from the first steady value to the second steady value. In contrast, Fig. 4C shows typical results, here termed pattern B.  $I_{\text{calcein}}$  did not increase and  $I_{\text{AF647}}$  remained constant during the interaction up to 6 min, indicating that PGLa did not enter the GUV lumen and no pore formation occurred in the GUV membrane. The  $\delta$  of the GUV rapidly increased to a steady value of  $\delta_1$  at 60 s, and then remained constant up to 6 min. Of 10 GUVs examined,

Figure 4

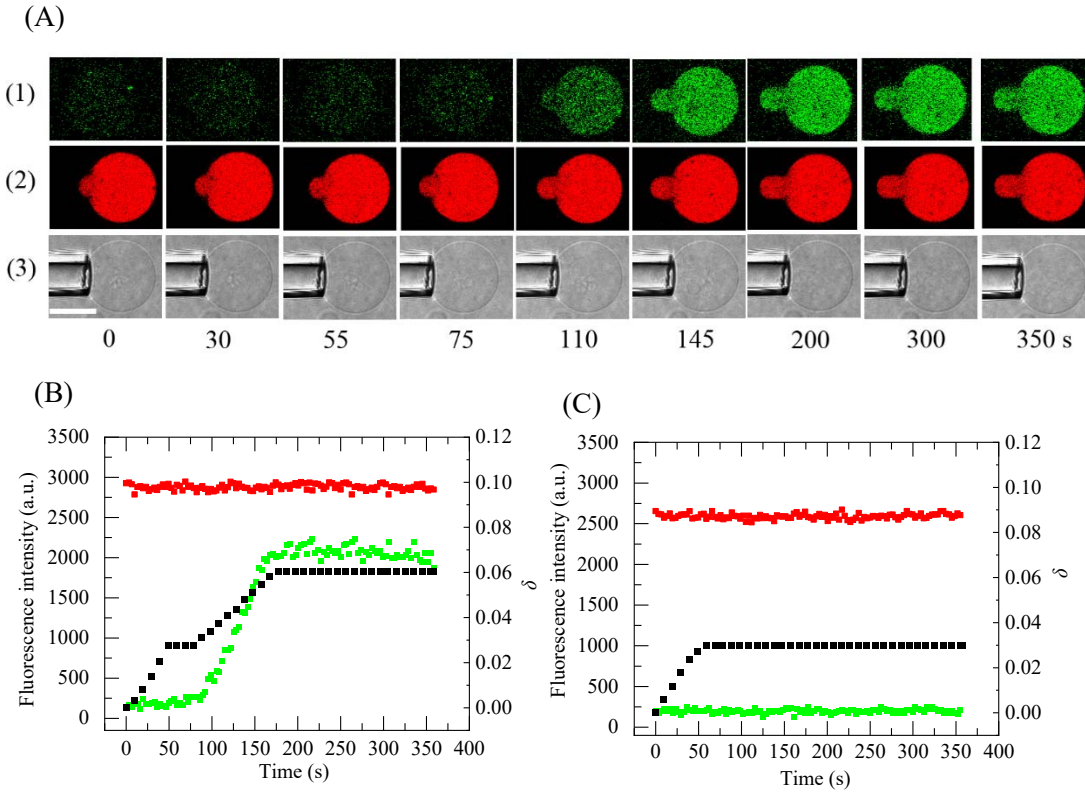


Figure 4. Simultaneous measurement of the PGLa-induced change in area of GUV membrane ( $\delta$ ) and the entry of PGLa into the GUV lumen. (A) CLSM images due to (1) calcein, (2) AF647, and (3) DIC image. A DOPG/DOPC (4/6)-GUV containing 10  $\mu$ M DOPG/DOPC (8/2)-LUVs (encapsulating high concentration of calcein) and AF647 was held at the tip of a micropipette (membrane tension was 0.5 mN/m) and was started to interact with 2.9  $\mu$ M PGLa at time = 0 s. The numbers below each image indicate the time of the interaction of PGLa with the GUV. Bar, 20  $\mu$ m. (B) Time course of change in FI of the GUV and  $\delta$  of the GUV shown in panel A. Green squares and red squares denote  $I_{calcein}$  and  $I_{AF647}$ , respectively (left axis). Black squares denote  $\delta$  (right axis). (C) Time course of change in FI of the GUV and  $\delta$  of another GUV. The symbols are the same in the panel B.

we obtained similar pattern A results (i.e., a two-step increase in  $\delta$  and an increase in  $I_{calcein}$  during the increase in  $\delta$ , without leakage of AF647) with 7 GUVs, whereas with the other 3 GUVs we obtained similar pattern B results (a one-step increase in  $\delta$  and no increase in  $I_{calcein}$ ). The average fraction of pattern A response was  $0.71 \pm 0.01$  ( $N = 2$ ), and thus,  $P_{entry}(6 \text{ min}) = 0.71 \pm 0.01$  ( $N = 2$ ). The mean value and SD of  $\delta_2/\delta_1$  was  $2.2 \pm 0.2$  ( $n = 17$  for  $N = 2$ ), and the mean value and SD of the time required from the first steady value to the second steady value of the  $\delta$  was  $99 \pm 15$  s. The difference between the onset time in increase in  $I_{calcein}$  (i.e.,  $t_o(I_{calcein})$ ) and that

of the increase in  $\delta$  from the first steady value (i.e.,  $t_o(\delta)$ ), i.e.,  $t_o(I_{\text{calcein}}) - t_o(\delta)$ , is  $20 \pm 10$  s ( $n = 17$  for  $N = 2$ ), indicating that  $I_{\text{calcein}}$  started to increase  $\sim 20$  s later than the onset time of increase in  $\delta$ . On the other hand, the difference between the termination time in increase in  $I_{\text{calcein}}$  (i.e.,  $t_t(I_{\text{calcein}})$ ) and that of the increase in  $\delta$  from the first steady value (i.e.,  $t_t(\delta)$ ), i.e.,  $t_t(I_{\text{calcein}}) - t_t(\delta)$ , is  $2 \pm 10$  s ( $n = 17$  for  $N = 2$ ), indicating that both termination times are similar.

The above results indicate that the increase in  $I_{\text{calcein}}$  occurs only when the fractional area change of the GUV membrane increases from the first steady value ( $\delta_1$ ) to the second steady value ( $\delta_2$ ). These findings can be explained as follows. First, PGLa binds to the membrane interface of the outer leaflet of a GUV, increasing the area of the GUV membrane. This binding reaches equilibrium rapidly, after which no change occurs for an extended period. Then, suddenly, PGLa starts to gradually translocate across the lipid bilayer from the membrane interface of the outer leaflet to the inner leaflet. During this translocation, the PGLa concentration in the outer leaflet remains constant, because the binding equilibrium of PGLa between the aqueous solution and the outer leaflet exists and the rate constant of the binding of PGLa from aqueous solution to the outer leaflet is large. Moreover, the PGLa concentration in the aqueous solution of the vicinity of the target GUV remains constant in the single GUV method. Therefore, the translocation of PGLa to the inner leaflet increases the total PGLa concentration in the lipid bilayer, inducing further increase in the area of the GUV membrane. During the translocation of PGLa across the bilayer, PGLa transfers from the inner leaflet to the GUV lumen, resulting in its entry to the GUV lumen. In principle, this transfer decreases the PGLa concentration in the inner leaflet, concomitantly the decrease in the GUV area. However, this phenomenon was not observed. This can be explained as follows. The translocation and the entry of PGLa occur almost simultaneously, and the rate of translocation of PGLa from the outer leaflet to the inner leaflet is higher than that of the transfer of PGLa from the inner leaflet to the GUV lumen. Therefore, the transfer of PGLa decreases the rate of increase in PGLa concentration in the inner leaflet (i.e., the increase in GUV area). In other words, if the transfer of PGLa does not occur, we could observe more rapid increase in GUV area due to the translocation of PGLa. From a theoretical point of view, the area change of a spherical GUV on the asymmetric binding of peptides to the GUV (i.e., the peptides bind only to the outer leaflet and not to the inner leaflet) is smaller than that on the symmetric binding of peptides (i.e., the peptides bind to both the outer and the inner leaflets).<sup>42</sup> The asymmetric binding of

the peptides induces an increase in area of the outer leaflet, causing a stretch of the inner leaflet due to the constraint of the same area of two monolayers for a spherical GUV, and the resulting tension in the inner leaflet decreases the area of the GUV membrane. Based on this theory,<sup>42</sup> we can obtain that the fractional area change in the symmetric binding becomes double that in asymmetric binding (see the section S1 in the Supporting Information). This model can explain the obtained result that the PGLa-induced two-step increase in area and  $\delta_2/\delta_1$  is  $\sim 2$ . As described in the Introduction, the interaction of a mixture of PGLa and a very low concentration (0.15  $\mu\text{M}$ ) of CF-PGLa with single GUVs results in the rim intensity due to CF-PGLa increasing with time in a two-step manner: the peptide concentration increases to a steady value,  $C_1$ , which remains constant for an extended period, and then increases again to another steady value,  $C_2$ , without pore formation in the GUV membrane. The ratio of  $C_2$  to  $C_1$  (i.e.,  $C_2/C_1$ ) is  $\sim 2$  and does not change after pore formation, and the time courses of the increase in  $I_{\text{rim}}$  due to CF-PGLa and  $\delta$  due to PGLa are almost the same.<sup>24</sup> This result also supports the above interpretation that initially PGLa locates only in the outer leaflet and then suddenly begins to gradually translocate across the lipid bilayer from the membrane interface of the outer leaflet to that of the inner leaflet until its concentration in the inner and outer leaflets is equal. This translocation occurs during the increase in  $\delta$  from  $\delta_1$  to  $\delta_2$ . Following translocation, PGLa is rapidly transferred from the inner leaflet into the GUV lumen. This result suggests that the rate constant of unbinding of PGLa from the membrane interface is large. PGLa in the GUV lumen then interacts with the LUVs, inducing calcein leakage from the LUVs and an increase in  $I_{\text{calcein}}$  due to the dequenching of calcein fluorescence.

Next, we investigated the interaction of 3.8  $\mu\text{M}$  PGLa with single PG/PC (4/6)-GUVs using the same method. GUVs provided results belonging to the pattern A response: a two-step increase in  $\delta$  and an increase in  $I_{\text{calcein}}$  during the increase in  $\delta$ . Figure S4 shows an example. Figure S4B indicates that the  $\delta$  of the GUV rapidly increased to a steady value of  $\delta_1$  at 40 s and remained constant for an extended period (30 s). Then, at 70 s,  $\delta$  started to increase gradually and reached a second steady value of  $\delta_2$  at 157 s, which remained constant until the GUV was aspirated into the micropipette at 335 s due to pore formation in the GUV membrane. The ratio of  $\delta_2$  to  $\delta_1$  ( $\delta_2/\delta_1$ ) was 2.3. On the other hand,  $I_{\text{calcein}}$  started to increase at 82 s (the onset time in increase in  $I_{\text{calcein}}$ ), which is almost the same as the onset time of the increase in  $\delta$  from the first steady value. Then,  $I_{\text{calcein}}$

reached a steady value at 138 s (the termination time in increase in  $I_{\text{calcein}}$ ), which is 19 s earlier than the time when  $\delta$  reached the second steady value,  $\delta_2$  (the termination time in increase in  $\delta$ ) (Fig. S4B). These results indicate that PGLa enters the GUV lumen when the GUV membrane area increases from the first steady value to the second steady value. Of 7 GUVs examined, we obtained similar pattern A results (i.e., a two-step increase in  $\delta$  and an increase in  $I_{\text{calcein}}$  during the increase in  $\delta$ , without leakage of AF647) with all GUVs. Based on 3 independent experiments ( $N = 3$ ), the fraction of pattern A response was 1.0, and thus,  $P_{\text{entry}}(6 \text{ min}) = 1.0$ . The mean values and SDs of  $\delta_2/\delta_1$  and  $\delta_1$  were  $2.3 \pm 0.2$  and  $0.0029 \pm 0.003$ , respectively ( $n = 25$  for  $N = 3$ ). The mean value and SD of the time required from the first steady value to the second steady value of  $\delta$  was  $87 \text{ s} \pm 12 \text{ s}$ . The difference between the onset time in increase in  $I_{\text{calcein}}$  and that of the increase in  $\delta$  from the first steady value, i.e.,  $t_o(I_{\text{calcein}}) - t_o(\delta)$ , is  $13 \pm 7 \text{ s}$  ( $n = 25$  for  $N = 3$ ), indicating that  $I_{\text{calcein}}$  started to increase  $\sim 13 \text{ s}$  later than the onset time of increase in  $\delta$ . On the other hand, the difference between the termination time in increase in  $I_{\text{calcein}}$  and that of the increase in  $\delta$  from the first steady value, i.e.,  $t_t(I_{\text{calcein}}) - t_t(\delta)$ , is  $-27 \pm 15 \text{ s}$  ( $n = 25$  for  $N = 3$ ), indicating that  $I_{\text{calcein}}$  stopped to increase  $\sim 27 \text{ s}$  earlier than the termination time of increase in  $\delta$ . This result may suggest that after PGLa concentration in the GUV lumen reaches  $2.0 \mu\text{M}$  (inducing 100% leakage of calcein from the LUVs) the PGLa concentration continues to increase, resulting in a further increase in  $\delta$ . Some GUVs were aspirated into the micropipette after the fractional area of the GUV membrane reached the second steady value ( $\delta_2$ ). Aspiration was due to PGLa-induced pore formation, followed by the membrane tension due to micropipette aspiration, resulting in rupturing of the GUV and its aspiration into the micropipettes due to the pressure difference.<sup>40</sup> The fraction of ruptured GUVs at 6 min was 0.56 ( $N = 3$ ), which is the same as  $P_{\text{leak}}(6 \text{ min})$  and the fraction of PGLa-induced pore formation.

### 3.4. Effect of membrane tension on entry of nonlabeled PGLa into GUV lumen

Examining the effects of membrane tension on the action of AMPs and CPPs is useful in elucidating their mechanism of action.<sup>43</sup> We used almost the same method as in section 3.3 but applied various membrane tensions to individual GUVs using different suction pressures. The peptide concentration was  $1.7 \mu\text{M}$  PGLa because this concentration provides a low  $P_{\text{entry}}(6 \text{ min})$  of 0.30 in the absence of tension. First, we examined

Figure 5

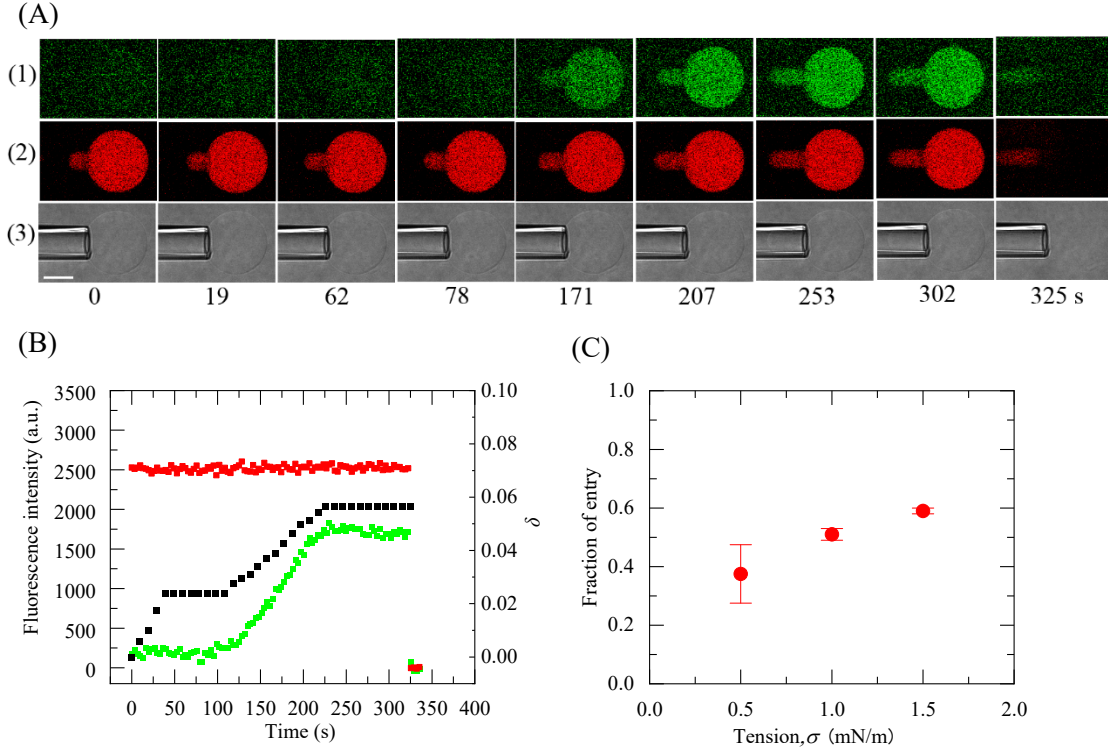


Figure 5. Effect of membrane tension on the entry of PGLa into the GUV lumen. (A) CLSM images due to (1) calcein, (2) AF647, and (3) DIC image. A DOPG/DOPC (4/6)-GUV containing 10  $\mu$ M DOPG/DOPC (8/2)-LUVs (encapsulating high concentration of calcein) and AF647 was held at the tip of a micropipette (membrane tension was 1.5 mN/m) and was started to interact with 1.7  $\mu$ M PGLa at time = 0 s. The numerals below each image indicate the time of the interaction of PGLa with the GUV. Bar, 20  $\mu$ m. (B) Time course of change in FI of the GUV and  $\delta$  of the GUV shown in panel A. Green squares and red squares denote  $I_{calcein}$  and  $I_{AF647}$ , respectively (left axis). Black squares denote  $\delta$  (right axis). (C) Membrane tension dependence of the fraction of entry of PGLa.

the effect of 1.5 mN/m on the interaction of 1.7  $\mu$ M PGLa with single GUVs. Figures 5A and 5B indicate that the  $\delta$  of the GUV rapidly increased to a steady value of  $\delta_1$  within 39 s, then remained constant for an extended period ( $\sim 70$  s). Then, at 110 s,  $\delta$  started to increase gradually and reached a second steady value of  $\delta_2$  at 226 s, which remained constant until the GUV was aspirated into the micropipette at 325 s due to pore formation. The ratio of  $\delta_2$  to  $\delta_1$  ( $\delta_2/\delta_1$ ) was 2.3. On the other hand,  $I_{calcein}$  did not increase at the beginning of the interaction but started to increase at 120 s, slightly later than the onset time of the increase in  $\delta$  from the first steady value.

Then,  $I_{\text{calcein}}$  reached a steady value at 230 s, later than the time when  $\delta$  reached the second steady value,  $\delta_2$  (Fig. 5B). We repeated these experiments using 12 GUVs and obtained a  $P_{\text{entry}}$  (6 min) value of 0.58.

We also repeated the same experiments using different membrane tensions. Figure 5C shows that  $P_{\text{entry}}$  (6 min) increased with membrane tension, indicating that the rate of entry of PGLa into single GUV lumens increased with increasing membrane tension. The fraction of ruptured GUVs at 6 min also increased with an increase in membrane tension (0 at 0.5 mN/m, 0.34 at 1.0 mN/m, and 0.50 at 1.5 mN/m). This result indicates that the rate of PGLa-induced pore formation increased with increasing membrane tension.

#### 4. General Discussion

In this study, we found that nonlabeled PGLa translocates across the lipid bilayer of a GUV from its outer leaflet to its inner leaflet and enters the GUV lumen without pore formation in the GUV membrane. This entry occurs only when the fractional area change of the GUV membrane increases from the first steady value to the second steady value, i.e., when PGLa translocates from the outer leaflet to the inner leaflet. The fraction of entry of PGLa increases with an increase in PGLa concentration and membrane tension. These results indicate that PGLa has the same translocation characteristics as CPPs. We previously demonstrated that a fluorescent probe-labeled PGLa (CF-PGLa) can enter the GUV lumen as the area of the GUV membrane increases from the first steady value to the second steady value.<sup>24</sup> However, the present study clearly indicates that labeling with a fluorescent probe is not required for the entry of the peptide. PGLa is an AMP and attacks bacterial cells without labeling with probes. The results presented here using a nonlabeled peptide are thus more significant than those obtained using fluorescent probe-labeled peptides. The labeling of CPPs with fluorescent probes is reported to change their interaction with cells.<sup>25,26</sup> The results presented in this and our previous report<sup>24</sup> indicate that the labeling of PGLa with CF does not change the translocation of the peptide across the lipid bilayer or its entry into the GUV lumen.

As described in the Introduction, there are two possible interpretations of the two-step increase in  $\delta$ . In interpretation A, a structural change in PGLa induces the observed two-step increase in  $\delta$ , whereas in interpretation B, the translocation of PGLa from the outer leaflet to the inner leaflet induces the two-step increase in  $\delta$ .<sup>22</sup> Here, we consider which interpretation is more valid given the results in this report. Figure S2

provides information on the PGLa concentration in a GUV lumen if we assume that the PGLa-induced increase in  $I_{\text{calcein}}$  of the GUV lumen is the same as that of the LUV suspension interacting with PGLa.<sup>35</sup> At and above 2.0  $\mu\text{M}$  PGLa, the FI values of the LUV suspension reached a saturated value of  $2300 \pm 100$ . As described in section 3.2, the mean values and SDs of the steady values of  $I_{\text{calcein}}$  of single GUVs interacting with 2.9  $\mu\text{M}$  and 3.8  $\mu\text{M}$  PGLa were  $2,800 \pm 300$  and  $2,700 \pm 400$ , respectively. Two factors cause fluctuations in  $I_{\text{calcein}}$ : (i) the efficiency of the entrapment of LUVs in a GUV lumen ( $81 \pm 10\%$ ), inducing  $\pm 13\%$  error in the LUV concentration in the GUV lumen, and (ii) the fluctuation of the radius of the GUVs, inducing an error in the position of the focal plane above the cover slip.<sup>35</sup> If we take these errors into account, we can conclude that the steady values of  $I_{\text{calcein}}$  of single GUVs are similar to the saturated FI values of the LUV suspension. These results therefore suggest that the PGLa concentration in the lumen of single GUVs interacting with 2.9  $\mu\text{M}$  and 3.8  $\mu\text{M}$  PGLa is above 2.0  $\mu\text{M}$ , which supports that following entry, the PGLa concentration in the GUV lumen is high. Since the equilibrium binding of PGLa from the aqueous solution in the GUV lumen to the inner leaflet of the GUV is maintained, it is difficult to infer that PGLa locates only in the outer leaflet (i.e., PGLa does not locate in the inner leaflet) after a significant concentration of PGLa enters the GUV lumen. Therefore, the results in this study clearly indicate that PGLa locates not only in the outer leaflet but also in the inner leaflet (i.e., PGLa distributes symmetrically) without pore formation, supporting the validity of interpretation B. Furthermore, we obtained theoretically that the fractional area change of a GUV membrane induced by the symmetric binding of peptides to both leaflets of the GUV becomes double that induced by asymmetric binding of peptides to only the outer leaflet based on a new theory.<sup>42</sup> This theoretical conclusion agrees with the experimental result that the PGLa-induced two-step increase in area and  $\delta_2/\delta_1$  is  $\sim 2$ . This agreement also supports the validity of interpretation B.

There is a large correlation between the increase in  $\delta$  from  $\delta_1$  to  $\delta_2$  (due to the translocation of PGLa across the lipid bilayer) and the entry of PGLa into the GUV lumen (Fig. 3). Thus, we can reasonably infer that the time courses of the entry of PGLa shown in Figs. 2C, 2D, and 2E are essentially the same as those of the translocation of PGLa across the lipid bilayer in the absence of membrane tension. The results shown in Figs.

2C, 2D, and 2E therefore indicate that the translocation of PGLa across the lipid bilayer occurs stochastically and the rate of translocation of PGLa increases with increasing PGLa concentration.

It is important to compare the interaction of fluorescent probe-labeled PGLa (i.e., CF-PGLa) and nonlabeled PGLa with the GUVs. In the interaction of a mixture of nonlabeled PGLa and a very low concentration of CF-PGLa (e.g., the total concentration of 2.9  $\mu\text{M}$  including 0.15  $\mu\text{M}$  CF-PGLa) with single GUVs,<sup>24</sup> in some GUVs during these peptides (mainly PGLa)-induced increase in area of GUV membrane from the first steady value to the second steady value of the  $\delta$ , CF-PGLa translocates from the outer leaflet to the inner leaflet, and then immediately enters the GUV lumen. The fraction of GUVs where the two-step increase in  $\delta$  is observed for 6 min among all examined GUVs, which is the same as the fraction of entry for 6 min ( $P_{\text{entry}}(6 \text{ min})$ ), is 0.47. In this report, in the interaction of nonlabeled PGLa (e.g., 2.9  $\mu\text{M}$ ) with single GUVs, in some GUVs during PGLa-induced increase in  $\delta$  from its first steady value to its second steady value, PGLa translocates from the outer leaflet to the inner leaflet, and then immediately enters the GUV lumen. The fraction of GUVs where the two-step increase in  $\delta$  is observed for 6 min among all examined GUVs and the value of  $P_{\text{entry}}(6 \text{ min})$  are 0.71. Hence, the behaviors of CF-PGLa and PGLa are qualitatively the same in this regard. On the other hand, we do not have any experimental data of only CF-PGLa-induced pore formation in lipid bilayers and only CF-PGLa-induced area change of GUV membrane. Therefore, it is difficult to compare quantitatively the rate of pore formation induced by two peptides and the fractional area change of the GUV membrane induced by two peptides. We can reasonably expect that the attachment of hydrophobic fluorescent probe affects the binding constant of peptides to lipid bilayers and the rate of peptide-induced pore formation quantitatively. It is reported that the rate constant of CF-TP10-induced pore formation is  $\sim 3$  times larger than that of nonlabeled TP10.<sup>44</sup>

The entry of CPPs into the cytosol of cells and the lumen of lipid vesicles are well known. Especially, the entry of the CPP TP10 into a GUV lumen has been extensively examined.<sup>35,37,38,44</sup> Thus, it is instructive to compare the mode of entry of PGLa and that of TP10. At low peptide concentrations, both nonlabeled peptides enter the GUV lumen without pore formation. At higher peptide concentration they enter the GUV lumen and after a long lag time pore formation occurs. Comparing the elementary processes by which both peptides enter the GUV lumen requires the use of fluorescent probe-labeled peptides. With TP10, the time course of the FI of

a GUV membrane (i.e., rim intensity) indicates that immediately after CF-TP10 begins to interact with a single GUV, the peptide concentration in the GUV membrane increases monotonically with time until it reaches a steady, maximum, value, not changing even after pore formation.<sup>37,44</sup> This indicates that CF-TP10 translocates from the outer leaflet to the inner leaflet from the beginning of the interaction until the peptide concentration in the two leaflets becomes equal at the maximum peptide concentration in the membrane (i.e., a symmetric distribution of the peptide in the membrane). The time course of the CF-TP10-induced increase in the fractional area change is similar to that of the increase in peptide concentration in the GUV membrane.<sup>45</sup> The entry of CF-TP10 into the GUV lumen starts when the CF-TP10 concentration in the GUV membrane approaches its maximum value at low peptide concentrations.<sup>38,46</sup> In contrast, after CF-PGLa begins to interact with a single GUV, the CF-PGLa concentration in the GUV membrane increases with time in two steps. The time course of the PGLa-induced increase in fractional area change is similar to that of the increase in peptide concentration in the GUV membrane, and the ratio of  $\delta_2$  to  $\delta_1$  (i.e.,  $\delta_2/\delta_1$ ) is approximately 2.<sup>24</sup> As described in the section 3.3, we can conclude that PGLa locates only in the membrane interface of the outer leaflet (i.e., asymmetric binding), and then after a lag time, PGLa translocates to the inner leaflet to reach the same surface concentration in both leaflets (i.e., symmetric binding). PGLa enters the GUV lumen as the area of GUV membrane increases from the first steady value to the second steady value, that is, during the translocation of CF-PGLa from the outer to the inner leaflet.<sup>24</sup> The largest difference between the translocation of PGLa and TP10 is that TP10 can immediately translocate continuously from the outer leaflet to the inner leaflet but PGLa is first located only in the outer leaflet for an extended time and then suddenly begins to translocate from the outer leaflet to the inner leaflet. This translocation continues for 50–150 s, depending on the peptide concentration, and the onset time of translocation is different for each GUV.

Here, we consider the mechanism of translocation of PGLa and its subsequent entry into the GUV lumen. CPPs are remarkable for their translocation across lipid and cell membranes and thus are the subject of much research. There are several models for the translocation of CPPs across lipid membranes.<sup>27–31,46</sup> In the pore model, CPPs interact with lipid membranes and induce a pore, and then permeate through the pore to enter the GUV lumen.<sup>47–49</sup> A pore is generally defined as a water channel through which small water-soluble fluorescent probes such as AF647 can permeate. Since the Stokes-Einstein radius of AF647 is estimated as 0.9 nm,<sup>50</sup> here

the pore is defined as the water channel with more than 0.9 nm radius. In contrast, the interaction of PGLa with GUVs results in no pore formation in the GUV membrane and thus the pore model is not appropriate to explain the translocation of these peptides. In the inverted micelle model, cationic CPPs bind with anionic lipids stoichiometrically to form an inverted micelle.<sup>51-53</sup> In the pre-pore model,<sup>38,45,46,54</sup> CPPs diffuse through a pre-pore, i.e., a nanodomain with a lower lipid density in the membrane produced tentatively by thermal fluctuation in the membrane in the liquid-crystalline phase.<sup>55-57</sup> The outer and the inner monolayers are believed to bend strongly to connect with each other in a pre-pore and thus the pre-pore wall has high positive curvature and its surface is composed of the hydrophilic regions of the lipids (i.e., the toroidal structure). The pre-pore wall has high free energy per unit length of the rim, called the line tension, and thus the lifetime of a pre-pore is very short. When an amphipathic CPP binds to the membrane interface of the outer monolayer of a GUV, it can bind to the pre-pore wall immediately after pre-pore formation if it locates near the pre-pore. This binding may decrease its free energy due to a decrease in line tension, which stabilizes the pre-pore and thus its lifetime increases. During this extended lifetime, the peptide can diffuse laterally along the connected monolayer at the pre-pore wall from the outer to the inner monolayer.<sup>46</sup> This pre-pore model can explain the translocation of PGLa and TP-10 across the lipid bilayer without pore formation. The theory describing tension-induced pore formation in lipid bilayers suggests that as the stretching of the lipid bilayer increases or the membrane tension increases, the energy barrier or the activation energy for pore formation decreases, which increases the rate constant of both pore formation<sup>55-57</sup> and pre-pore formation.<sup>43,45</sup> Thus, the rate of translocation of PGLa across the lipid bilayer increases with an increase in membrane tension, which reasonably explains the results shown in Fig. 5C. The binding of PGLa to only the outer leaflet (i.e., asymmetric binding) induces stretching of the inner leaflet of the GUV membrane, as demonstrated with magainin 2.<sup>40,43</sup> This increases the rate of pre-pore formation, inducing an increase in the rate of translocation of PGLa across the lipid bilayer. We currently do not know how the pre-pore model can explain the different modes of translocation of these peptides, i.e., the gradual translocation of TP10 and the sudden, cooperative translocation of PGLa. We hypothesize that TP10 can permeate through small pre-pores, whereas PGLa can permeate through only larger pre-pores. The radius of a pre-pore is believed to fluctuate due to thermal force.<sup>55,56</sup> Small pre-pores appear frequently but larger ones appear rarely. Only a larger thermal fluctuation of the lipid bilayer can produce such a large pre-pore, and thus

the large pre-pore is formed rarely and stochastically. This inference can reasonably explain the experimental results that the translocation of PGLa across the lipid bilayer occurs rarely and stochastically. We suggest that if a large pre-pore forms, PGLa starts to translocate across the lipid bilayer, and then PGLa continues to translocate across the lipid bilayer through some cooperative translocation mechanism until the PGLa concentration in the inner leaflet becomes equal to that in the outer leaflet. Further studies in the near future are required to elucidate the cooperative translocation mechanism.

Ulmschneider conducted MD simulation results on PGLa<sup>34</sup> and showed that PGLa translocates across a dimyristoyl-phosphatidylglycerol (DMPG)/dimyristoyl-phosphatidylcholine (DMPC) (1/3) membrane as rapidly as across a DMPC membrane without pore formation (on a time scale of tens of microseconds per peptide). Two or three peptides form a transient complex via a water bridge at the N-terminal region of the peptides, and then one peptide converts to the S-state in the inner leaflet (i.e., it translocates to the inner leaflet) and other peptides return to the S-state in the outer leaflet. In contrast, our experimental results show that PGLa localizes in the outer leaflet at the same peptide concentration for an extended period (50–200 s), corresponding to the first steady state with a constant value of  $\delta_1$  before translocation begins. The MD simulation results cannot explain the first steady state or the lag time between when the peptide concentration in the outer leaflet reaches a steady value and the onset of translocation, since in the MD simulation, peptide translocation begins immediately.<sup>34</sup> The disadvantage of current all-atom MD simulations is that they cannot provide information on the thermal fluctuations of lipid bilayer structures such as pre-pore formation due to their limited duration and the small membrane area (i.e., the small number of lipids) used in the simulation.<sup>58</sup>

As described in the Introduction, PGLa is classified as a type A AMP (its antimicrobial activity or bactericidal activity is due largely to the damage it causes to the plasma membrane of bacterial cells, resulting in significant leakage of the internal cell contents). However, the results in this report clearly indicate that low concentrations (1.7–2.9  $\mu\text{M}$ ) of PGLa can enter the GUV lumen without pore formation in the GUV membrane, suggesting that low concentrations of PGLa behave as either a type B or CPP-type AMP. At low concentrations, PGLa may enter the cytosol of bacterial cells without damaging the plasma membrane and then bind to important biomolecules such as DNA and proteins, thereby causing cell death.<sup>2,10</sup> Confirming this hypothesis

will require investigating the interaction of PGLa with single bacterial cells and single spheroplasts in the near future.<sup>8,10</sup>

## 5. Conclusion

Here we demonstrated that nonlabeled PGLa enters the lumen of a DOPG/DOPC (4/6)-GUV without pore formation in the GUV membrane, indicating clearly that nonlabeled PGLa can translocate from the membrane interface of the outer leaflet to that of the inner leaflet. At and above 1.7  $\mu\text{M}$  PGLa, the fraction of entry of PGLa into the GUV lumen is enhanced as the peptide concentration increases. We found that the interaction of PGLa with single GUVs induces a two-step increase in the fractional area change of the GUV membrane ( $\delta$ ) and PGLa enters the GUV lumen only during the second increase in  $\delta$ . The fraction of entry of PGLa without pore formation increases with increasing membrane tension, indicating that membrane tension enhances the rate of translocation of PGLa across the lipid bilayer and that of entry into the GUV lumen. These results provide insights into the elementary processes and mechanism of the translocation of PGLa across the GUV membrane and its entry into the GUV lumen.

## Acknowledgements

This work was supported in part by a Grant-in-Aid for Scientific Research (B) (No. 19H03193) from the Japan Society for the Promotion of Science (JSPS) to M.Y. This work was also supported in part by the Cooperative Research Project of the Research Center for Biomedical Engineering. We appreciated Dr. Farzana Hossain and Md. Masum Billah for their critical reading of this manuscript, and Dr. Md. Mamun Or Rashid for his technical assistance.

## Supporting Information (SI)

The data of entry of PGLa into a single GUV interacting with 3.8  $\mu\text{M}$  PGLa, the data of the CLSM measurement of the FI of the LUV suspensions interacting with various concentrations of PGLa, the data of the interaction of 2.9  $\mu\text{M}$  PGLa with single DOPG/DOPC (8/2)-GUVs containing DOPG/DOPC (8/2)-LUVs, the data of the

simultaneous measurement of the 3.8  $\mu$ M PGLa-induced change in area of GUV membrane ( $\delta$ ) and the entry of PGLa into the GUV lumen, and the theory of the binding of peptides-induced area change of a GUV membrane.

## REFERENCES

- (1) Zasloff, M. Antimicrobial peptides of multicellular organisms. *Nature*. **2002**, *415*, 389-395.
- (2) Brogden, K. A. Antimicrobial peptides: pore formers or metabolic inhibitors in bacteria? *Nat. Rev. Microbiol.* **2005**, *3*, 238-250.
- (3) Hancock, R. E. W.; Hans-Georg, S. Antimicrobial and host-defense peptides as new anti-infective therapeutic strategies. *Nat. Biotech.* **2006**, *24*, 1551-1557.
- (4) Melo, M. N.; Ferre, R.; Castanho, A. R. B. Antimicrobial peptides: linking partition, activity and high membrane-bound concentrations, *Nat. Rev. Microbiol.* **2009**, *8*, 1-5.
- (5) Matsuzaki K (ed), Antimicrobial Peptides: Basic for Clinical Application, **2019**, Springer Nature.
- (6) Propheter, D. C.; Chara, A. L.; Harris, T. A.; Ruhn, K. A.; Hooper L. V. Resistin-like molecule  $\beta$  is a bactericidal protein that promotes spatial segregation of the microbiota and the colonic epithelium, *Proc. Natl. Acad. Sci. U.S.A.* **2017**, *114*, 11027-11033.
- (7) Sochacki, K.A.; Barns, K. J.; Bucki, R.; Weisshaar, J. C. Real-time attack on single *Escherichia coli* cells by the human antimicrobial peptide LL-37. *Proc. Natl. Acad. Sci. U.S.A.* **2011**, *108*, E77-E81.
- (8) Hossain, F.; Moghal, M. M. R.; Islam, M. Z.; Moniruzzaman, M.; Yamazaki, M. Membrane potential is vital for rapid permeabilization of plasma membranes and lipid bilayers by the antimicrobial peptide lactoferricin B. *J. Biol. Chem.* **2019**, *294*, 10449-10462.
- (9) Park, C. B.; Yi, K. -S.; Matsuzaki, K.; Kim, M. S.; Kim, S. C. Structure-activity analysis of buforin II, a histone H2A-derived antimicrobial peptide: The proline hinge is responsible for the cell-penetrating ability of buforin II. *Proc. Natl. Acad. Sci. U.S.A.* **2000**, *97*, 8245-8250.
- (10) Hossain, F.; Hideo Dohra, H.; Yamazaki, M. Effect of membrane potential on entry of lactoferricin B-derived 6-residue antimicrobial peptide into single *Escherichia coli* cells and lipid vesicles. *J. Bacteriology*, **2021**, *203*, e00021-21.

- (11) Hoffmann, W.; Richter, K.; Kreil, G. A novel peptide designated PYL<sup>a</sup> and its precursor as predicted from cloned mRNA of *Xenopus laevis* skin, *EMBO J.* **1983**, *2*, 711-714.
- (12) Giovannini, M. G.; Poulter, L.; Gibson, B. W.; Williams, D. H. Biosynthesis and degradation of peptides derived from *Xenopus laevis* prohormones, *Biochem. J.* **1987**, *243*, 113-120.
- (13) Latal, A.; Degovics, G.; Epand, R. F.; Epand, R. M.; Lohner, K. Structural aspects of the interaction of peptidyl-glycylleucine-carboxyamide, a highly potent antimicrobial peptide from frog skin, with lipids, *Eur. J. Biochem.* **1997**, *248*, 938-946.
- (14) Lohner, K.; Prossnigg, F. Biological activity and structural aspects of PGLa interaction with membrane mimetic systems. *Biochim. Biophys. Acta - Biomembr.* **2009**, *1788*, 1656-1666.
- (15) Wieprecht, T.; Apostolov, O.; Beyermann, M.; Seelig, J. Membrane binding and pore formation of the antibacterial peptide PGLa; thermodynamic and mechanistic aspects, *Biochemistry* **2000**, *39*, 442-452.
- (16) Bechinger, B.; Zasloff, M.; Opella, S. J. Structure and dynamics of the antibiotic peptide PGLa in membranes by solution and solid-state nuclear magnetic resonance spectroscopy. *Biophys. J.* **1998**, *74*, 981-987.
- (17) Glaser, R. W.; Sachse, C.; Dürr, U. H. N.; Wadhwani, P.; Afonin, S.; Strandberg, E.; Ulrich, A. S. Concentration-dependent realignment of the antimicrobial peptide PGLa in lipid membranes observed by solid-state <sup>19</sup>F-NMR, *Biophys. J.* **2005**, *88*, 3392-3397.
- (18) Tremouihac, P.; Strandberg, E.; Wadhwani, P.; Ulrich, A. S. Conditions affecting the re-alignment of the antimicrobial peptide PGLa in membranes as monitored by solid state <sup>2</sup>H-NMR, *Biochim. Biophys. Acta*, **2006**, *1758*, 1330-1342.
- (19) Strandberg, E.; Tremouihac, P.; Wadhwani, P.; Ulrich, A. S. Synergistic transmembrane insertion of the heterodimeric PGLa/magainin 2 complex studied by solid state NMR, *Biochim. Biophys. Acta*, **2009**, *1788*, 1667-1679.
- (20) Williams, R. W.; Starman, R.; Taylor, K. M.; Gable, K.; Beeler, T.; Zasloff, M.; Covell, D. Raman spectroscopy of synthetic antimicrobial frog peptides magainin 2a and PGLa, *Biochemistry* **1990**, *29*, 4490-4496.

- (21) Vaz Gomes, A.; de Waal, A.; Berden, J. A.; Westerhoff, H. V. Electric potentiation, cooperativity, and synergism of magainin peptides in protein-free liposomes, *Biochemistry* **1993**, *32*, 5365-5372.
- (22) Matsuzaki, K.; Mitani, Y.; Akada, K.; Murase, O.; Yoneyama, S.; Zasloff, M.; Miyajima, K. Mechanism of synergism between antimicrobial peptides magainin 2 and PGLa, *Biochemistry* **1998**, *37*, 15144-15153.
- (23) Blazyk, J.; Wiegand, R.; Klein, J.; Hammer, J.; Epand, R. M.; Epand, R. F.; Maloy, W. L.; Kari, U. P. O. A novel linear amphipathic  $\beta$ -sheet cationic antimicrobial peptide with enhanced selectivity for bacterial lipids, *J. Biol. Chem.* **2001**, *276*, 27899-27906.
- (24) Parvez, F.; Alam, J. M.; Dohra, H.; Yamazaki, M. Elementary processes of antimicrobial peptide PGLa-induced pore formation in lipid bilayers. *Biochim. Biophys. Acta - Biomembr.* **2018**, *1860*, 2262-2271.
- (25) Birch, D.; Christensen, M. V.; Staerk, D.; Franzyk, H.; Nielsen, H. M. Fluorophore labeling of a cell-penetrating peptide induces differential effects on its cellular distribution and affects cell viability. *Biochim. Biophys. Acta - Biomembr.* **2017**, *1859*, 2483-2494.
- (26) Hedegaard, S. F.; Derbas, M. S.; Lind, T. K.; Kasimova, M. R.; Christensen, M. V.; Michaelsen, M. H.; Campbell, R. A.; Jorgensen, L.; Franzyk, H.; Cárdenas, M.; Nielsen, H. M. Fluorophore labeling of a cell-penetrating peptide significantly alters the mode and degree of biomembrane interaction. *Sci. Rep.* **2018**, *8*, 6327.
- (27) Magzoub, M.; Gräslund, A. Cell-penetrating peptides: small from inception to application. *Quart. Rev. Biophys.* **2004**, *37*, 147-195
- (28) Zorko, M.; Langel, Ü. Cell-penetrating peptides: mechanism and kinetics of cargo delivery. *Adv. Drug Delivery Rev.* **2005**, *57*, 529-545.
- (29) Madani, F.; Lindberg, S.; Langel, Ü.; Futaki, S.; Gräslund, A. Mechanisms of cellular uptake of cell-penetrating peptides. *J. Biophysics*, **2011**, 414729.
- (30) Koren, E.; Torchilin, V. P. Cell-penetrating peptides: breaking through to the other side. *Trends. Mole. Med.* **2012**, *18*, 385-393
- (31) Bechara, C.; Sagan, S. Cell-penetrating peptides: 20 years later, where do we stand? *FEBS. Lett.* **2013**, *587*, 1693-1702.

- (32) Leontiadou, H.; Mark, A. E.; Marrink, S. J. Antimicrobial peptides in action, *J. Am. Chem. Soc.* **2006**, *128*, 12156-12161.
- (33) Bennett, W. F. D.; Hong, C. K.; Wang, Y.; Tieleman, D. P. Antimicrobial peptide simulations and the influence of force field on the free energy for pore formation in lipid bilayers. *J. Chem. Theory Comput.* **2016**, *12*, 4524-4533.
- (34) Ulmschneider, J. P. Charged antimicrobial peptides can translocate across membranes without forming channel-like pores. *Biophys. J.* **2017**, *113*, 73-81.
- (35) Shuma, M. L.; Moghal, M. M. R.; Yamazaki, M. Detection of the entry of nonlabeled transportan 10 into single vesicles. *Biochemistry*, **2020**, *59*, 1780-1790.
- (36) Bartlett, G.R. Phosphorous assay in column chromatography. *J. Biol. Chem.* **1959**, *234*, 466-468.
- (37) Moghal, M. M. R.; Islam, M. Z.; Sharmin, S.; Levadnyy, V.; Moniruzzaman, M.; Yamazaki, M. Continuous Detection of Entry of Cell-Penetrating Peptide Transportan 10 into Single Vesicles. *Chem. Phys. Lipids*. **2018**, *212*, 120-129.
- (38) Moghal, M. M. R.; Islam, M. Z.; Hossain, F.; Saha, S. K.; Yamazaki, M. Role of Membrane Potential on Entry of Cell-Penetrating Peptide Transportan 10 into Single Vesicles. *Biophys. J.* **2020**, *118*, 57-69.
- (39) Tamba, Y.; Terashima, H.; Yamazaki, M. A membrane filtering method for the purification of giant unilamellar vesicles. *Chem. Phys. Lipids*, **2011**, *164*, 351-358.
- (40) Karal, M. A. S.; Alam, J. M.; Takahashi, T.; Levadny, V.; Yamazaki, M. Stretch-Activated Pore of Antimicrobial Peptide Magainin 2. *Langmuir*, **2015**, *31*, 3391-3401.
- (41) Rawicz, W.; Olbrich, K. C.; McIntosh, T.; Needham, D.; Evans, E. Effect of chain length and unsaturation on elasticity of lipid bilayers. *Biophys. J.* **2000**, *79*, 328-339.
- (42) Levadnyy, V.; Hasan, M.; Saha, S. K.; Yamazaki, M. Effect of transmembrane asymmetric distribution of lipids and peptides on lipid bilayers. *J. Phys. Chem. B*, **2019**, *123*, 4645-4652.
- (43) Hasan, M.; Moghal, M. M. R.; Saha, S. K.; Yamazaki, M. The role of membrane tension in the action of antimicrobial peptides and cell-penetrating peptides in biomembranes. *Biophys. Rev.* **2019**, *11*, 431-448.

- (44) Islam, M. Z.; Ariyama, H.; Alam, J. M.; Yamazaki, M. Entry of cell-penetrating peptide transportan 10 into a single vesicle by translocating across lipid membrane and its induced pores. *Biochemistry*, **2014**, *53*, 386-396.
- (45) Islam, M. Z.; Sharmin, S.; Levadnyy, V.; Shibly, S. U. A.; Yamazaki, M. Effects of Mechanical Properties of Lipid Bilayers on Entry of Cell-Penetrating Peptides into Single Vesicles. *Langmuir*. **2017**, *33*, 2433-2443.
- (46) Islam, M. Z.; Sharmin, S.; Moniruzzaman, M.; Yamazaki, M. Elementary Processes for the Entry of Cell-Penetrating Peptides into Lipid Bilayer Vesicles and Bacterial Cells, *Appl. Microbiol. Biotechnol.* **2018**, *102*, 3879-3892.
- (47) Mishra, A.; Gordon, V. D.; Yang, L.; Coridan, R.; Wong, G. C. L. HIV TAT forms pores in membranes by inducing saddle-spray curvature: potential role of bidentate hydrogen bonding. *Angew. Chem. Int. Ed.* **2008**, *47*, 2986-2989.
- (48) Ciobanasu, C.; Siebrasse, J. P.; Kubitscheck, U. Cell-penetrating HIV1 TAT peptides can generate pores in model membranes. *Biophys. J.* **2010**, *99*, 153-162.
- (49) Mishra, A., Lai, G. H., Schmidt, N. W., Sun, V. Z., Rodriguez, A. R., Tong, R., Tang, L., Cheng, J., Deming, T. J., Kamei, D. T., and Wong, G. C. L. Translocation of HIV TAT peptide and analogues induced by multiplexed membrane and cytoskeletal interactions, *Proc. Natl. Acad. Sci. U.S.A.*, **2011**, *108*, 16883-16888.
- (50) Hasan, M.; Saha, S. K.; Yamazaki, M. Effect of membrane tension on transbilayer movement of lipids. *J. Chem. Phys.* **2018**, *148*, 245101.
- (51) Berlose, J.-P.; Convert, O.; Derossi, D.; Brunissen, A.; Chassaing, G. Conformational and associative behaviors of the third helix of antennapedia homeodomain in membrane-mimetic environments. *Eur. J. Biochem.* **1996**, *242*, 372-386.
- (52) Kawamoto, S.; Takasu, M.; Miyakawa, T.; Morikawa, R.; Oda, T.; Futaki, S.; Nagao, H. Inverted micelles formation of cell-penetrating peptide studied by coarse-grained simulation: Importance of attractive force between cell-penetrating peptides and lipid head group. *J. Chem. Phys.* **2011**, *134*, 095103.

- (53) Swiecicki, J.-M.; Bartsch, A.; Tailhades, J.; Di Pisa, M.; Heller, B.; Chassaing, G.; Mansuy, C.; Burlina, F.; Lavielle, S. The efficacies of cell-penetrating peptides in accumulating in large unilamellar vesicles depend on their ability to form inverted micelles. *Chem. Bio. Chem.* **2014**, *15*, 884-891.
- (54) Sharmin, S.; Islam, M. Z.; Karal, M. A. S.; Shibly, S. U. A.; Dohra, H.; Yamazaki, M. Effects of lipid composition on the entry of cell-penetrating peptide oligoarginine into single vesicles. *Biochemistry.* **2016**, *55*, 4154-4165.
- (55) Evans, E.; Smith, B. A. Kinetics of hole nucleation in biomembrane rupture. *New J. Phys.* **2011**, *13*, 095010.
- (56) Levadny, V.; Tsuboi, T.; Belaya, M.; Yamazaki, M. Rate Constant of Tension-Induced Pore Formation in Lipid Membranes. *Langmuir.* **2013**, *29*, 3848-3852.
- (57) Akimov, S. A.; Volynsky, P. E.; Galimzyanov, T. R.; Kuzmin, P. I.; Pavlov, K. V.; Batishev, O. V. Pore formation in lipid membrane I: Continuous reversible trajectory from intact bilayer through hydrophobic defect to transversal pore. *Sci. Rep.* **2017**, *7*, 12152.
- (58) Buch, I.; Harvey, M. J.; Giorgino, T.; Anderson, D. P.; Fabritiis, G. D. High-throughput all-atom molecular dynamics simulations using distributed computing. *J. Chem. Inf. Model.* **2010**, *50*, 397-403.